



BACHELOR THESIS

GENOMIC PROFILING OF SEX-SPECIFIC DIFFERENCES IN AN OSTEOARTHRITIS-ON-CHIP MODEL

Design of organ-on-a-chip holder

Author:

Rianne Vos (s2288877)

Study:

Biomedical Technology

Daily supervisor:

Francisco Pereira dos santos Conceição

Chair supervisor:

Liliana Moreira Teixeira Leijten

External member:

Jeroen Leijten

Department:

Advanced Organ bioengineering and Therapeutics (AOT)

ENSCHEDA, JUNE 2023

UNIVERSITY OF TWENTE.

Acknowledgements

I would like to thank my supervisors for their guidance and support during the research project. First of all, I would like to thank my daily supervisor Francisco Pereira dos santos Conceição for the clear lab introductions and giving me the confidence to work on a lab on my own. He was always available and approachable, and his feedback was very useful during the project. I want to thank Liliana Moreiera Teixeira Leijten, for the opportunity to do research in her faculty, her enthusiasm on the project, and evaluating the thesis.

Abstract

Osteoarthritis (OA) is a complex musculoskeletal disease, and it affected 7% of the global population in 2019. Gender differences regarding OA have received limited research attention thus far, and further investigation is required to understand the underlying mechanisms. This study used an innovative organ-on-a-chip technology to explore gender differences in OA. In this way a more representative and physiological model was used compared to existing approaches.

To enable simultaneous perfusion of multiple chips, the design of a specialized holder was developed. This holder enhanced the research throughput and transportability of microfluidic systems. The chip-holder, waste tube holder, and baseplate were designed using SolidWorks software. The final design successfully achieved most of the intended aims and requirements. This offers promising possibilities for organs-on-chips perfusion experiments in the future. However, some minor limitations were observed, such as challenges in focusing cells under a microscope due to plate thickness and the stiffness of tubing causing slides to lift.

The newly designed holder was used for perfusion over three days with pro-inflammatory cytokines to obtain gene expression profiles of two donors with OA. The findings indicated potential differences in gene expression between men and postmenopausal women. The ESR1, IL-1 β , MMP9, and RANKL were expressed by the female donor but not by the male donor. Conversely, SP7 and TLR4 were expressed by the male donor and not by the female donor. However, the study had some limitations and emphasized the need for obtaining a larger group of donors to create more reliable evidence.

This study is part of a larger research project that involved the influence of inflammatory stimuli on the gene expression of osteoblast and chondrocyte cells. Moreover, the study's findings lay the foundation for a deeper understanding of gender differences in OA. This is crucial for the development of personalized and effective treatment strategies. Particularly because the global population ages and healthcare demands continue to rise.

Samenvatting

Osteoarthritis (OA) is een complexe aandoening aan het musculoskeletale stelsel wat 7% van de wereldbevolking trof in 2019. Geslachtsverschillen met betrekking tot OA hebben tot nu toe beperkte onderzoek aandacht gekregen en verder onderzoek is nodig om de onderliggende mechanismen te begrijpen. Deze studie maakte gebruik van de innovatieve orgaan-on-chip technologie om genderverschillen in OA te onderzoeken. Op deze manier wordt een representatiever en meer fysiologisch model gebruikt in vergelijking met bestaande modellen.

Om gelijktijdige perfusie van meerdere chips mogelijk te maken werd een gespecialiseerde houder ontworpen. Deze houder verbeterde de doorvoer en transporteerbaarheid van microfluidische systemen. De chip-houder, afvalbuis houder en basisplaat werden ontworpen met behulp van het software Solidworks. Het uiteindelijke ontwerp was succesvol en voldeed aan de meest doelen en vereisten. Dit biedt veelbelovende mogelijkheden voor experimenten met perfusie van organen-on-chips in de toekomst. Er werden echter enkele kleine beperkingen waargenomen, zoals uitdagingen bij het scherpstellen van cellen onder de microscoop vanwege de dikte van de plaat en de stijfheid van de verbindingdraden waardoor de platen omhoogkomen.

De nieuw ontworpen houder werd gebruikt voor perfusie gedurende drie dagen met pro-inflammatoire cytokines om genexpressieprofielen van twee donoren met OA te verkrijgen. De bevindingen wijzen op mogelijke gerelateerde verschillen in genexpressie tussen mannen en postmenopauzale vrouwen. De genen ESR1, IL-1 β , MMP9 en RANKL werden tot expressie gebracht door de vrouwelijke donor maar niet door de mannelijke donor. Omgekeerd werden SP7 en TLR4 tot expressie gebracht door mannelijke donor maar niet door de vrouwelijke donor. De studie heeft echter beperkingen en benadrukte de noodzaak om grotere groep donoren te gebruiken om betrouwbaarder bewijs te verkrijgen.

Deze studie maakt deel uit van een breder onderzoek, waarbij de invloed op inflammatoire stimuli op de genexpressie van osteoblast en chondrocyt cellen wordt onderzocht. Bovendien leggen de bevindingen van deze studie de basis voor een dieper begrip van geslachts-specifiek aspecten van OA. Een volledig begrip van geslachtsverschillen in OA is cruciaal voor de ontwikkeling van gepersonaliseerde en effectieve behandelingsstrategieën, vooral vanwege de vergrijzende wereldbevolking en de toenemende vraag naar de gezondheidszorg.

Index

Acknowledgements	
Abstract	
Samenvatting.....	
List of abbreviations	
1. Introduction.....	1
1.1. Articular cartilage	1
1.2. Cartilage disorders.....	2
1.3. Risk factors	3
1.4. Gene expression profiling.....	5
1.5. Model for osteoarthritis	5
2. Assignment.....	7
2.1. Aims and objectives.....	7
2.1.1. Aims of the holder	7
2.1.2. Objectives of the holder	7
2.1.3. Aims of the osteoarthritis-on-chip model	8
2.1.4. Objectives of the osteoarthritis-on-chip model	8
2.2. Hypothesis	8
3. Materials and Methods	9
3.1. Osteoarthritis-on-a-chip fabrication	9
3.2. Design process of the holder.....	9
3.3. Osteoarthritis-on-chip culture.....	11
3.3.1. Donors	11
3.3.2. Cell thawing.....	11
3.3.3. Microfluidic seeding	11
3.3.4. Preparation of microfluidic perfusion setup	12
3.3.5. Cell extraction of chips	12
3.3.6. RNA isolation and cDNA synthesis	12
3.3.7. RT-qPCR	12
4. Results of the holder	14
4.1. Define phase of the holder.....	14
4.2. Measure phase of the holder	15
4.3. Analyze phase of the holder	16
4.4. Design phase of the holder	19
4.4.1. Design of components.....	19
4.4.2. Product	19

5.	Results of the osteoarthritis-on-chip model	21
5.1.	Observations	21
5.2.	RNA isolation values	21
5.3.	Gene expression	22
5.4.	Perspectives of results.....	24
6.	Discussion.....	25
6.1.	The holder system	25
6.1.1.	Verify phase of the holder.....	25
6.1.2.	Future perspectives of the holder	26
6.2.	The osteoarthritis-on-chip model	27
6.2.1.	Challenges	27
6.2.2.	Future perspectives of the osteoarthritis-on-chip experiments	28
7.	Conclusion	30
8.	References.....	31
9.	Appendix.....	35
9.1.	The holder system	35
9.1.1.	Specifications of pump	35
9.1.2.	Specification of organ-on-chips direction	35
9.1.3.	Concept development	36
9.1.4.	Material choices	38
9.1.5.	Production drawing of each compartment	39
9.1.6.	Final product.....	41
9.1.7.	Revision on list-of-requirements.....	42
9.1.8.	Translation to industrial design	44
9.2.	The osteoarthritis-on-chip model	45
9.2.1.	Medium composition	45
9.2.2.	qPCR primers and plate layout.....	46

List of abbreviations

ADAMTS	A disintegrin and metalloproteinase with thrombospondin-like motifs
BOM	Bill-Of-Material
cDNA	Complementary deoxyribonucleic acid
CPC	Chondrogenic progenitor cell
Col	Collagen
ECM	Extracellular matrix
E2	Estradiol
FBS	Fetal bovine serum
IGF	Insulin like growth factor
IL	Interleukin
LAP	Lithium phenyl phosphinate
MMP	Matrix metalloproteinase
N	Sample size
nanoHA	Nano hydroxyapatite
OA	Osteoarthritis
OOC	Organ-on-a-chip
PBS	Phosphate-buffered saline
PDM	Proinflammatory differentiation medium
PDMS	Polydimethylsiloxane
PMMA	Polymethylmethacrylate
PVC	Polyvinyl chloride
RNA	Ribonucleic acid
RT-qPCR	Quantitative real-time polymerase chain reaction
TGF	Transforming growth factor
TLR	Toll-like receptor
TNF	Tumor necrosis factor
VEGF	Vascular endothelial growth factor

1. Introduction

The world's population is ageing, leading to a growing number of people living with chronic diseases and injuries [1]. Among these, musculoskeletal disorders have the highest prevalence, affecting approximately 1.71 billion people worldwide. Musculoskeletal disorders include a range of conditions that impact joints, bones, muscles, and various body areas or systems. Within musculoskeletal disorders, osteoarthritis (OA) is believed to be the most prevalent [1, 2]. In 2019, over 530 million people, 7% of the global population, were affected by OA [3]. As life expectancy and obesity rates of the global population continue to rise, the prevalence of OA is expected to increase significantly, along with high healthcare costs [2, 4, 5]. In recent years, it has become evident that gender plays a significant role in the development of OA. However, the existing knowledge and studies in this area remain limited [5, 6]. Therefore, the focus of this research is to investigate gender differences in OA using organ-on-a-chip technology. Starting with the healthy state of articular cartilage.

1.1. Articular cartilage

In our bodies, cartilage serves as a highly specialized connective tissue with the primary function of covering and safeguarding the ends of long bones. This provides protection against mechanical damage. Its structure is characterized by a dense extracellular matrix (ECM) that plays a crucial role in confining the movement of chondrocytes, the cells within cartilage. The ECM network contains thin collagen II fibers with a solution of proteoglycans, water and (glycol)proteins. The combination of fluid and solid matrix in a complex structure contributes to unique mechanical properties of articular cartilage. Unlike other tissues, cartilage is devoid of blood vessels, lymphatics, and nerves. The lack of vascularization and neural innervation results in a limited capacity of healing and repair processes within cartilage [7].

Cartilage is primarily composed of chondrocytes, specialized cells responsible for secreting the ECM [2, 7]. Chondrocytes are derived from mesenchymal stem cells and make up only 2% of the total adult cartilage volume [7]. However, their shape, number, and size vary depending on the region of articular cartilage (see Figure 1). The articular cartilage can be divided into three distinct zones. The superficial zone acts as a protective layer for the deeper zones and consists of flatter, smaller, and relatively densely packed chondrocytes. The middle layer contains fewer chondrocytes and can resist compressive forces. In contrast, the deep zone with larger and rounder chondrocytes can withstand compressive loads. Together, these zones ensure a homogeneous distribution of mechanical load and provide resistance against compression and shear forces created by the body [7, 8].

Within the articular cartilage, a layer of calcified cartilage separates it from the underlying subchondral bone plate. The calcified cartilage plays an important role in cartilage degradation, which is a major factor in OA development. Unlike cartilage, the subchondral bone is vascularized and innervated. It contains osteoblast cells that deposit a matrix rich of hydroxyapatite crystals. The complex structure of articular cartilage, combined with limited healing and restoration capacity, resulting in challenges in the repair process [9].

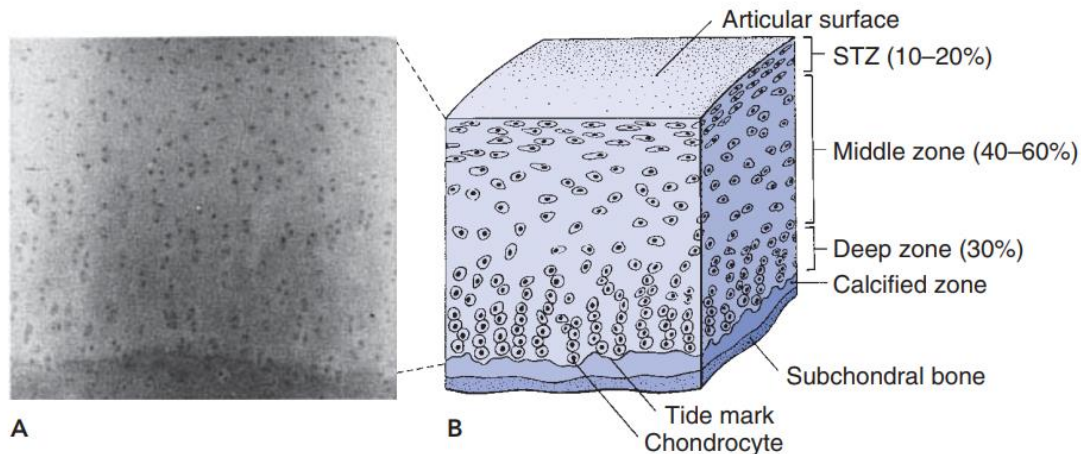


Figure 1. Structure of articular cartilage. (A) Histologic section of cartilage from a young, healthy adult showing the arrangement of chondrocytes. (B) Schematic diagram of chondrocyte organization of articular cartilage in three zones; superficial zone (STZ), middle zone, and deep zone. With the calcified layer between articular cartilage and subchondral bone plate [8].

Under normal conditions, articular chondrocytes and subchondral osteoblasts experience mechanical load and strain, which is an important function [9]. In physical activities the joint generates loads that are transmitted via the ECM to the chondrocytes, triggering cellular responses and activities [8]. However, in abnormal situations, such as repetitive and excessive joint overloading or high compressive stress, the cellular activity of the cells alters, which can lead to cartilage disorders [9].

1.2. Cartilage disorders

Arthritis is a collective name for joint disorders with common symptoms including swelling, inflammation, stiffness, and reduced range of motion. There are more than one hundred different types of arthritis, with osteoarthritis being the most prevalent form [1].

Common characteristics of OA include erosion in articular cartilage, tissue hypertrophy, vascular infiltration, instability of tendons and ligaments, and loss of subchondral bone (Figure 2A) [2]. The subchondral layer becomes weaker over time, leading to the development of osteophytes and bone cysts, which can be seen in Figure 2B [10]. Simultaneously, the degeneration of synovial joint contributes to the experience of pain and decreased mobility [11]. The activation of chondrocytes plays a role in this process, as they undergo phenotypic shifts, apoptosis, or abnormal gene expression (Figure 2B) [10]. The chondrocytes secrete multiple inflammatory proteins and cytokines, such as interleukin (IL), tumor necrosis factor (TNF), matrix-degrading enzymes of metalloproteinase (MMP), and a disintegrin and metalloproteinase with thrombospondin-like motifs (ADAMTS). Certain proteins seem to have crucial pathogenetic effects in OA, contributing to the inflammatory response and tissue breakdown. Some important signaling pathways and structural changes have been identified, as shown in Figure 3. However, the specific underlying pathways of OA are still not completely understood [12].

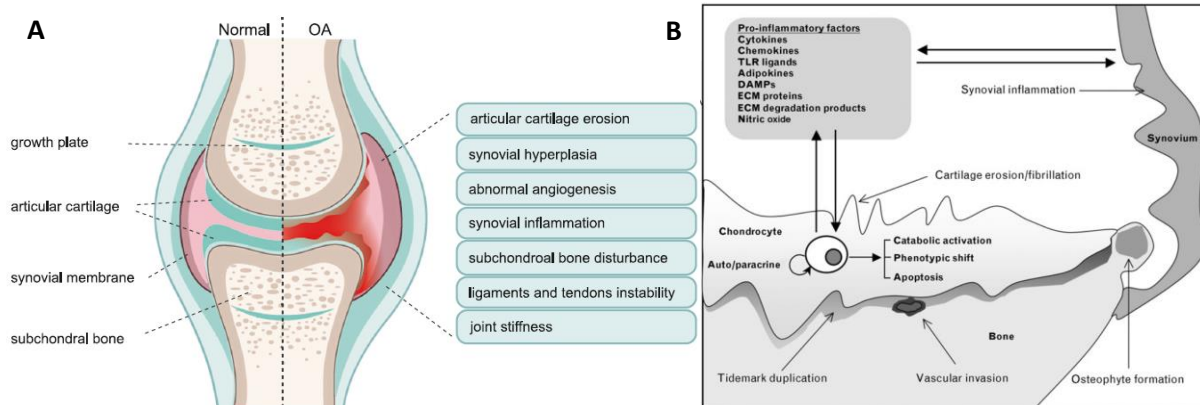


Figure 2. Pathogenesis of osteoarthritis. (A) Phenotypes of osteoarthritis patients with articular cartilage erosion, synovial hyperplasia, abnormal angiogenesis, synovial inflammation, subchondral bone disturbance, ligament and tendons instability, and joint stiffness. The left side shows the structure of normal synovial knee joint, while the right side shows possible alterations in the synovial structure affected by OA [2]. (B) Key mediators involved in the inflammatory processes of OA [10].

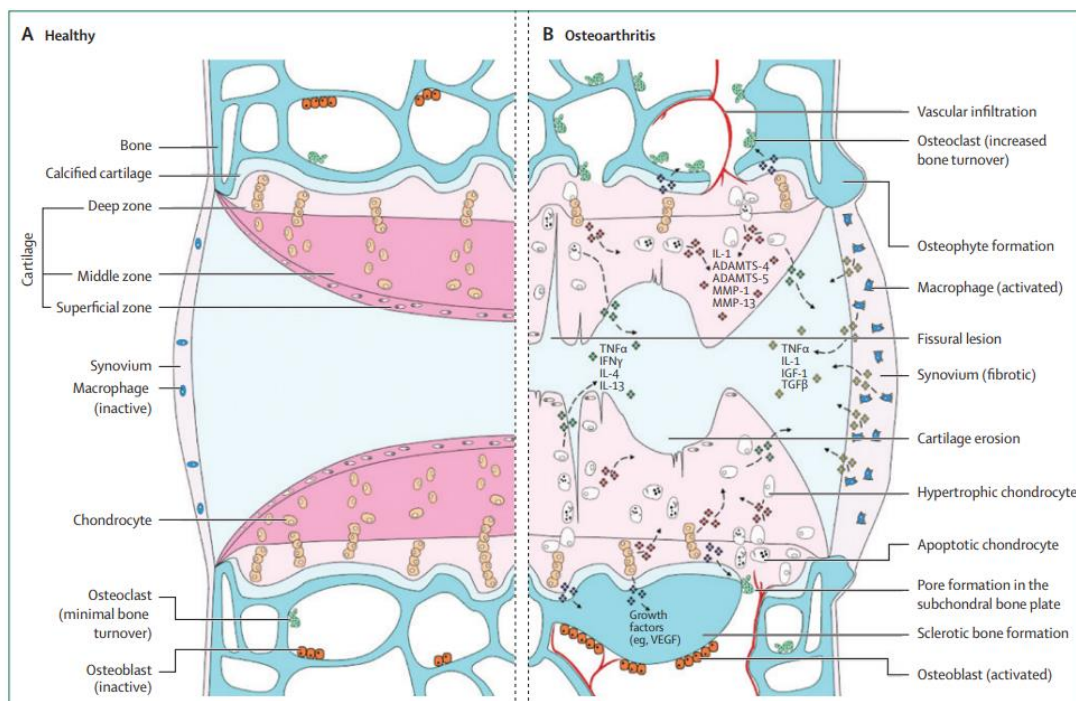


Figure 3. Signaling pathways and structural changes are involved in the development of osteoarthritis. The abbreviations used in the figure are as follows: ADAMTS (a disintegrin and metalloproteinase with thrombospondin-like motifs), IL (interleukin), MMP (matrix metalloproteinase), TNF (tumor necrosis factor), IGF (insulin-like growth factor), TGF (transforming growth factor), and VEGF (vascular endothelial growth factor) [12].

1.3. Risk factors

Osteoarthritis, being a complex multi-joint disease, is influenced by some risk factors. Important risk factors associated with OA include obesity, ageing, knee injuries, ethnicity, engaging in high-impact sports, and gender [2, 13, 14]. Among these factors, ageing has been identified as the highest risk factors, with one in three people over the age of 65 suffering from OA [15]. Over the past decade, it has become evident that gender also plays a significant role in the development of OA. However, the large knowledge gap, particularly at the molecular level, can be related to the lack of studies and preclinical models [6]. Nevertheless, it is observed that OA tends to affect women more than men [13, 15-17].

Studies have indicated that woman contain a higher incidence of hand, hip, and knee OA compared to men, especially from the age of 45 onwards [17, 18]. The incidence of knee and hip OA consistently increases with age for both genders, while hand OA peaks around the time of menopause in woman [17]. The gender difference in prevalence can be observed globally. Data from the Institute for Health Metrics and Evaluation shows the prevalence and incidence number of OA. They demonstrated that in The Netherlands between 1990 and 2019, almost twice the number of women were diagnosed with OA compared to men [3].

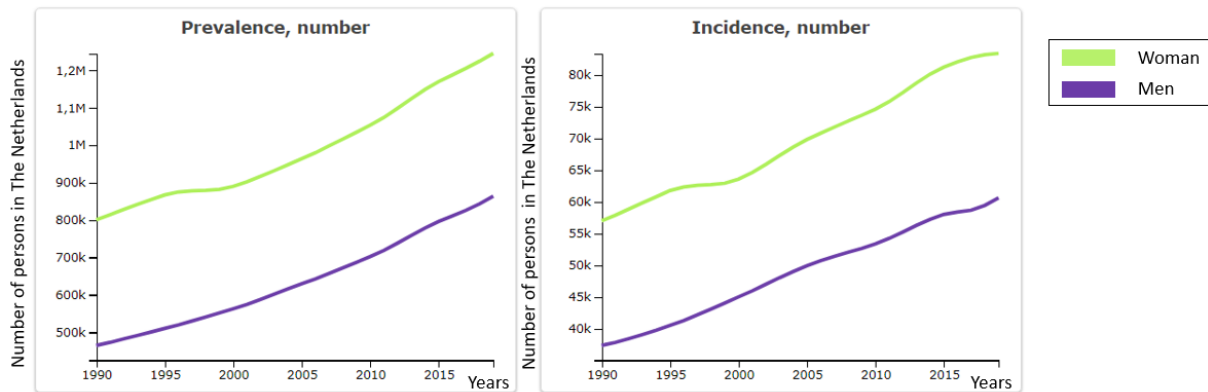


Figure 4. Prevalence and incidence of osteoarthritis in The Netherlands between 1990 and 2019. (A) The graph shows the number of OA prevalence cases over the last decades in The Netherlands. (B) The graph shows the number of OA incidence cases over the same period. It is evident that OA affect women (green) more than men (purple). The data presented in Figure 4 is extracted from the website <http://ghdx.healthdata.org/gbd-results-tool> [3].

Gender disparities in OA may be caused by differences in bone strength, pregnancy, and neuromuscular strength. Studies have reported that females display higher level of joint inflammation and may have a reduced volume of knee cartilage [19, 20]. Research has shown increased rates of cartilage loss and progression of cartilage defects in women’s knees. The annual rate of losing articular cartilage in the proximal tibia is four times higher, and in the patella three times higher, compared to men [21].

Particularly in the postmenopausal phase of women, there is higher incidence of OA compared to premenopausal women and men [22]. Reduced level of circulating sex hormones in postmenopausal women has been suggested as a potential trigger for development of the disease [21]. In postmenopausal women, the ovaries stop with the production of estradiol and progesterone [23, 24]. However, the role of hormones in correlation with gender disparity in cartilage loss is still not fully understood. Nevertheless, it can be concluded that the age of women, specifically after the menopausal phase, changes the hormone level which has a crucial role in OA development [21].

Women can be divided in pre- and postmenopausal groups, with postmenopausal females defined as those aged 55 or above. This subgroup is particularly interesting to investigate as they are more affected by OA [25]. Thus, in this research, our focus is on examining differences in gene expression between men and postmenopausal women, where the role of hormones is not included. For the sake of convenience, the term “women” in this report refers to postmenopausal women.

1.4. Gene expression profiling

Genes and hormones are widely characterized mediators of gender differences in immune responses [24]. Analyses of injured articular cartilage have revealed the activation and expression of specific cytokines and chemokines, like IL-6 and CCL2. Furthermore, chondrocytes have been observed to migrate to the injured side and express VEGF, RUNX2, and MMP13, resulting in the formation of a thicker cortical plate [26].

Klein et al.[24] found a relationship between hormones and gene expression in gender. Low doses of estradiol in postmenopausal women increased the production of pro-inflammatory cytokines IL-1 β , IL-6, and TNF [24]. In a separate study analyzing inflammatory cytokines measured in human synovial fluid they found higher level of MMP1, MMP9, MMP13, and TGF β 1 in men, while CSF and TNF were higher in woman. No significant differences were observed for IL-18 and IL-1 β [13]. These findings contradict the results found in rats, where a higher expression of IL-1 β was observed in synovial membranes of females [27]. Additionally, a larger study of TGF β 1 in serum reported higher level in women [28]. The expression of insulin-like growth factor genes, IGF1 and IGRFR1, in condylar cartilage was significantly lower in female rats. The same was found for Col2 [29]. Research on toll-like receptor pathways found that TLR7 gene can lead to higher expression levels in females compared to males [30]. Additionally, higher levels of TLR4 have been found in neutrophils of men [31]. The TLR9 showed stimulation in peripheral blood mononuclear cells of males, resulting in greater production of IL-10 compared to females [32].

Studying gene expression patterns is crucial for developing personalized strategies and improving diagnostic techniques in healthcare. It also provides valuable insight for designing gender-based approaches in physical rehabilitation programs and developing gender-specific drugs [5].

1.5. Model for osteoarthritis

Over the years, several models have been developed to study OA, including animal models, 2D, and 3D *in vitro* tissue models. While these models have provided valuable insights into the pathology and pathways of the disease, they have a limitation in translational power for evaluating therapies and predicting effectiveness [33]. These models fail to fully replicate the human cartilage, including its tissue structure, physiological conditions, and dynamic culture environment [34].

In recent years, organ-on-a-chip technology has been demonstrated as a promising alternative to animal testing for drug screening and disease modeling. These microfluidic devices allow cell culture in chambers of micrometer size and can be continuously perfused. Technology facilitates the miniaturization of organs by replicating their microenvironment, mechanics, and physiological condition [35]. Organ-on-a-chip can reproduce the multicellular architecture and tissue-tissue interfaces that are essential for studying complex diseases like OA [33].

Numerous organ-on-a-chip models have already been developed, including models for alveoli, lung airways, and heart tissues. These complex systems can contain multiple microchambers connected by microchannels through porous membranes. This way interfaces between different tissues can be created [35]. In OA, the interface between osteoblast and chondrocyte (the osteochondral barrier) plays an important role in the degradation process. This process can be stimulated by the addition of pro-inflammatory cytokines (IL-1 β and TNF α) to the perfusion medium flowing through the channels. This approach allows for the mimicking of synovial inflammation, seen in human OA [36].

By using organ-on-a-chip technology, we can overcome the limitation of existing models and create a more representative method for studying OA [33]. This approach provides the opportunity to investigate interaction between chondrocytes and osteoblasts in microscale environment [36].

In our research, we used a similar osteochondral unit-on-a-chip, as shown in Figure 5. Only an extra pillar was added to the design for separating the chondrocytes from the osteoblasts. To enable the perfusion of multiple chips at the same time, an organ-on-a-chip platform can be developed. This can increase the efficiency of organ-on-a-chip research.

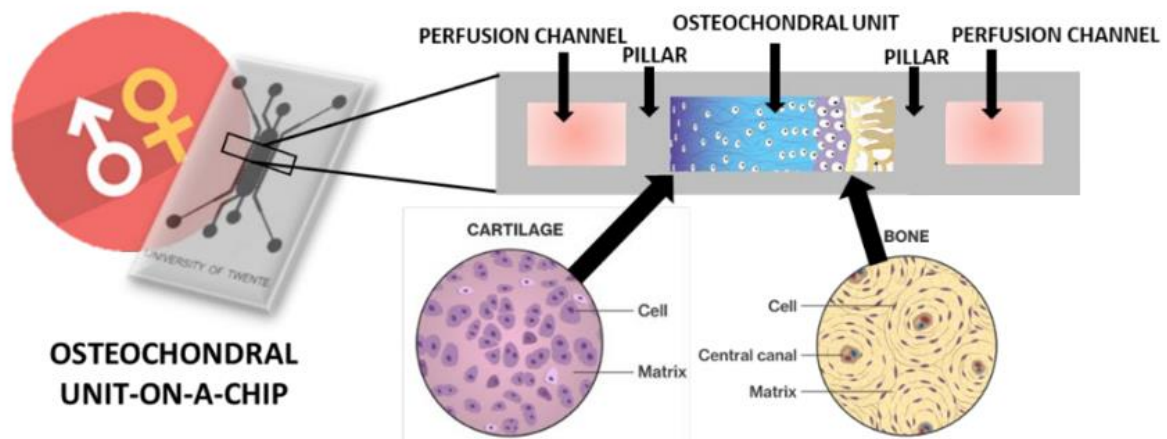


Figure 5. Osteochondral unit-on-a-chip which can mimic the human osteochondral barrier. On the left side the cartilage with chondrocyte cells in a matrix and on the right side the bone with osteoblasts in a matrix. Two continuous perfused channels with pro-inflammatory differentiation medium. The pillars resulting in connection of the perfusion channel and the cells. The figure is created with the Biorender app.

2. Assignment

This bachelor thesis comprises two main assignments. The first assignment involves the design of an organ-on-a-chip holder, which is a technical task. This provides the experimental setup for the second assignment, focused on the genomic profiling of sex-specific differences in osteoarthritis. Different techniques will be necessary to perform the experiments, such as microfabrication of microfluidic chips, design processes, cell culture techniques, and gene expression analyses using real time qPCR. The supervision team for this thesis consists of Dr. L. Moreira Teixeira and Dr. F. Conceição from the Advanced Organ bioengineering and Therapeutics (AOT) department of the University of Twente.

2.1. Aims and objectives

The primary research question of this study is to identify genomic profiling of sex-specific differences in an osteoarthritis-on-chip model, specifically between men and postmenopausal women. This information will provide valuable insight into osteoarthritis disease, which can be useful for developing effective personalized strategies and improving diagnostic techniques [5].

To address the research question, several experiments will be performed. The research will be focused on differential expression of specific biomarkers present in chondrocytes and osteoblasts cells of two donors. A predefined set of biomarkers will serve as a base for building up an osteoarthritis-on-chip gender profile using RT-qPCR.

2.1.1. Aims of the holder

The aim of the holder design is to create a functional system that can accommodate multiple chips within an incubator for several days. This system should be transportable, user-friendly, and increase the throughput of perfused chips. It should improve the overall functionality and efficiency of the perfusion experiments.

In this research, the holder will be used as a perfusion system to gradually supply the osteoarthritis-chips with pro-inflammatory differentiation medium. In each experiment, the holder will last for three days inside an incubator. However, the holder can also be used for other perfusion setup experiments.

2.1.2. Objectives of the holder

In order to achieve the aim described above, the following objectives have been formulated for the holder design:

- Increase the throughput of organs-on-chips.
- Facilitate easier transport of microfluidics.
- Maintain the syringe pump, tubing and microfluidic chips leveled to avoid high pressure differences during perfusion.
- Minimize dead volume in the tubing by placing the chips and syringes close together.
- Collect conditioned media from each individual perfusion channel.
- Provide independent accessibility of components.
- Ensure long-term utilization of the holder.

2.1.3. Aims of the osteoarthritis-on-chip model

Currently, the importance of the gender role in osteoarthritis is underestimated, despite evidence indicating gender differences [5]. Therefore, the aim is to investigate the genetic profile of men and postmenopausal women in osteoarthritis and determine if there is a difference in gene expression. The designed holder will be utilized for perfusion experiments of three days, where five osteoarthritis-on-a-chip will be used to mimic the human osteochondral barrier.

2.1.4. Objectives of the osteoarthritis-on-chip model

In order to achieve the aim described above, the following objectives have been formulated:

- Conduct analyses of osteoarthritis using a microfluidic chips perfusion system for a duration of three days.
 - Establish a mineralized compartment of bone with osteoblasts and non-mineralized compartment of cartilage with chondrocytes.
 - Induce an inflammation response by applying pro-inflammatory cytokines to promote a diseased condition.
- Investigate the differences in gene expression between men and postmenopausal women.
 - Determine if there is a pattern visible in gene expression between genders.
 - Evaluate the disparities in gene expression.

2.2. Hypothesis

The hypothesis of this study is based on suggestions that the relation between inflammation markers and osteoarthritis may differ between postmenopausal women and men. Although existing literature is limited, a potential gender-related contrast in inflammation levels is indicated. Higher inflammation is observed in females compared to males [24]. Furthermore, most matrix metalloproteinases (MMPs) [13], toll-like receptors (TLRs) [31, 32], and insulin like growth factors (IGFs) have found to be higher expressed in men [29]. By investigating these gender-specific differences in an osteoarthritis-on-chip the bases can be set for understanding the underlying mechanisms of gender specificity in OA [36].

3. Materials and Methods

This section provides an overview of the materials and methods employed in the osteoarthritis-on-chip experiments. It includes the fabrication of a microfluidic device, the design of the experimental setup, and the osteoarthritis culture. The culture process is divided into cell thawing, microfluidic seeding, and preparation of the microfluidic setup. Subsequently, the section covers cell extraction from the chips, RNA isolation, cDNA synthesis, and RT-qPCR analyses. To visualize the overall process of culturing of the osteoarthritis-on-chip model, a schematic flowchart is presented in Figure 9.

3.1. Osteoarthritis-on-a-chip fabrication

The chips were fabricated using polydimethylsiloxane (PDMS; SYLGARD 184 Silicone Elastomer Kit) in which the base resin and curing agent were mixed in a 10:1 weight-to-weight ratio. Approximately 25 mL of mixed PDMS solution was cast onto a silicon mold provided in the University of Twente (Figure 6A). For this research, only the double compartment chips were utilized (see Figure 6B). The PDMS solution layer was degassed in a vacuum desiccator to eliminate air bubbles, and then cured in an oven at 65°C for 2 hours. Subsequently, the crosslinked PDMS layer was carefully peeled off from the silicon mold. The PDMS layer was first cut into individual chips, and then two types of ports were punched. Four ports with a diameter of 1.0 mm were punched to serve as inlets for cell culture media, indicated by red dots in Figure 6C. Additionally, four ports with a diameter of 1.5 mm were punched to serve as inlets for the culture chambers, indicated by green dots in Figure 6C. To covalently bond the chips on a microscope slide (VWR), both parts were exposed to oxygen plasma for 40 sec at 20 W using a Femto Science plasma device. Afterward, the chips were flipped with the microfluidic part facing downwards and pressed onto the microscope slide in pairs. Finally, the chips were covered with tape and stored before use in cell culture.

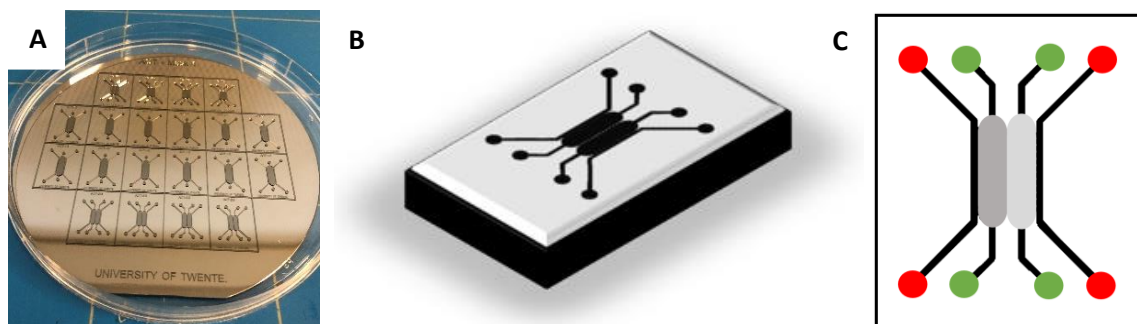


Figure 6. Geometry of osteoarthritis-on-chip device. (A) Silicon mold, created by Dr. F. Conceição, was used for the fabrication of chips. Only the first and fourth row of double compartments, were used in this research. (B) 3D representation of osteochondral unit-on-chips with double perfusion channels. (C) 2D top view of the osteochondral unit-on-chip, showing the perfusion ports in red and hydrogel ports in green. The left compartment (dark grey) contained osteoblast cells in a mineralized hydrogel network, while the right compartment (light grey) contained chondrocyte cells in non-mineralized hydrogel network. An intermediate boundary layer was present, allowing for interaction between the two cell types.

3.2. Design process of the holder

The design of the holder followed a five-step Design for Six Sigma methodology, consisting of the Define, Measure, Analyze, Design, and Verify (DMADV) steps, as depicted in Figure 7. This design process focused on the development of a new product [37]. In the “Define” step, the problem was explained in detail, and the goals were set. In the “Measure” step, the user’s requirements were determined, resulting in a complete list of requirements. In “Analyze” step, different concepts were generated in SolidWorks. The best design was selected, and a complete assembly of the total holder was created in SolidWorks.

Furthermore, the “Design” step explained the conversion of the best design into a prototype. A production drawing of each component was created in SolidWorks. The individual parts were manufactured in the workshop of the University of Twente. They were cut into square shapes and milled to achieve precise dimensions and features. Hole locations were marked and drilled. The assembly was performed using pins and screws. The final product was then transferred to the biological lab, cleaned with ethanol, and made ready for the experiments. In the last step, “Verify,” was the prototype validated to ensure its intended functions aligned with the defined requirements. Possible improvements were discussed.

The manufacturing process in the design step was conducted by R. Vos and supported by R. Beltman. Various techniques used in the fabrication process can be observed in Figure 8.

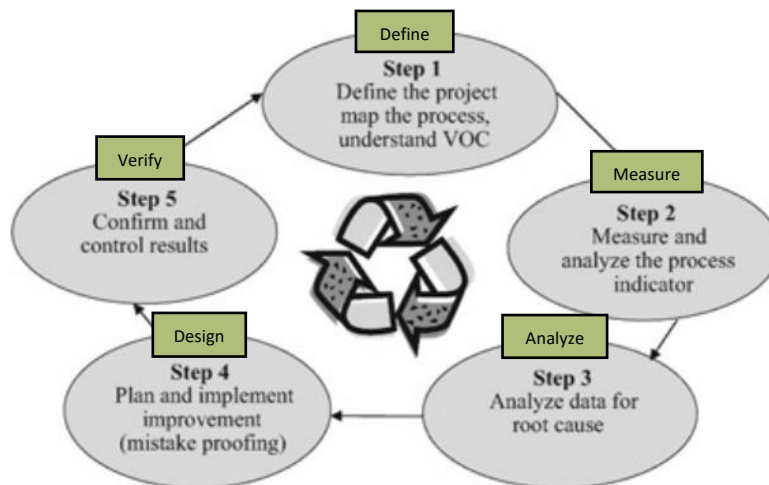


Figure 7. Five steps of Six Sigma methodology with Define, Measure, Analyze, Design, and Verify. These steps were used in the design process of the holder. Abbreviation of VOC (vision, output, and customer). The figure of Pocha et al.[37] was adjusted with green blocks to clarify the steps.

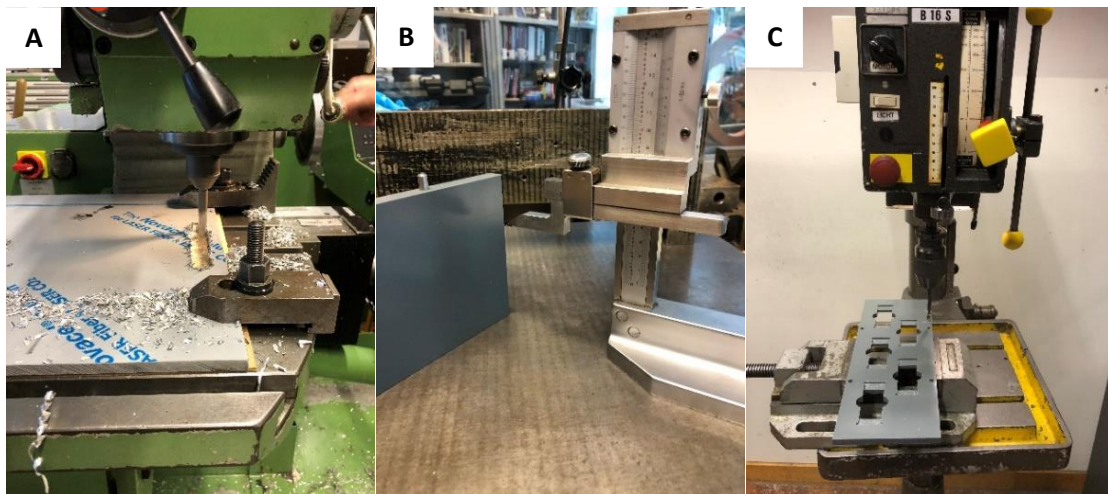


Figure 8. Most of production techniques were used in the fabrication process of the holder. (A) A milling machine was used to manufacture the parts with precise dimensions and features. (B) A drawing pencil was used to mark the correct drilling and spots for assembling the components. (C) A drilling machine was employed to create holes with the exact diameter.

3.3. Osteoarthritis-on-chip culture

3.3.1. Donors

Human osteoblasts and chondrocytes were separately isolated from surgical waste obtained from postmenopausal females and males. The osteoblasts were collected from fibula used in jaw reconstruction surgery, while the chondrocytes were collected from cartilage during knee arthroplasty surgery. The isolation of each cell type was performed by previous researchers and is not included in this report. The cells up to passage four were used. All cells were stored in liquid nitrogen (-196°C). One female donor and one male donor were analyzed using the following protocols.

3.3.2. Cell thawing

The osteoblasts and chondrocytes from the specific donor were defrosted at 37°C and refreshed with proliferation medium (Appendix 9.2.1, Table 8). Subsequently, the cells were centrifuged at 300 g for 3 min, the supernatant was aspirated, and the cells were resuspended with 1 mL of proliferation medium. They were separately seeded in a T75 flask (Thermo Fisher Scientific) with 10 mL of corresponding proliferation medium (Appendix 9.2.1, Table 8). Both flasks were incubated in a humidified incubator at 5% CO₂ and 37°C for 7 days. The medium was refreshed every 3 to 4 days. Confluence observations were performed using an EVOS microscope (Thermo Fisher Scientific).

3.3.3. Microfluidic seeding

Before microfluidic seeding, the chips were incubated in the oven for several hours to restore the hydrophobicity of the bonded surfaces and facilitate hydrogel handling. The osteoblasts and chondrocytes in the flasks were washed with Phosphate-Buffered Saline (PBS) and trypsinized in the incubator for 5 min. Meanwhile, the chips were sterilized for 15 min using a UV lamp source (36 W, Nail gel UV Lamp Evershine).

Each cell suspension was transferred to a tube and centrifuged for 3 min at 300 g. The supernatant was aspirated, and the cells were resuspended with proliferation medium (Appendix 9.2.1, Table 8). The number of cells was determined by the EVE Automated Cell Counter (NanoEnTek Inc). A cell suspension of 2×10^6 cells/mL was added to a new tube and then centrifuged for 3 min at 300 g.

For osteoblast seeding, the hydrogel was prepared using 8% GelMA (CELLINK), 0.2% (w/v) of photoinitiator Lithium Phenyl Phosphinate (LAP) (Sigma-Aldrich), and 0.5% (w/v) of nano Hydroxyapatite (nanoHA) (Sigma-Aldrich). The nanoHA was sonicated for 50 min before preparing the mineralized GelMA. The supernatant from the osteoblasts was removed, and the cells were resuspended in the mineralized GelMA solution and inserted into the respective compartment of the chip. The GelMA was photo-crosslinked by exposing the chips to UV light for 1.30 min.

For chondrocyte seeding, the GelMA solution was prepared using 8% GelMA and 0.2% LAP. The chondrocytes were resuspended in the GelMA solution, which was inserted into the respective compartment of the chip. The osteoblast compartment was covered with aluminum foil to prevent extra UV light exposure. The chips were again photo-crosslinked with UV light for 1.30 min. Differentiation medium was added on the respective perfusion channel.

The remaining cell suspensions were passaged in 10 mL proliferation medium in a T75 culture flask at a density of 3300 cells/cm². They were cultured in a 37°C humidified incubator with 5% CO₂ and refreshed with medium every 3 to 4 days.

3.3.4. Preparation of microfluidic perfusion setup

50 mL of osteoblast and chondrocyte differentiation medium was prepared (Appendix 9.2.1, Table 9). In new tubes (Falcon) was the differentiation medium supplemented with 10 ng/mL of proinflammatory cytokines IL-1 β and TNF α (Preprotech). Needles were inserted in the sterile 3 mL syringes and filled with proinflammatory differentiation medium (PDM), with half of the syringes containing osteoblast PDM and another half containing chondrocyte PDM. The holder with chips, syringes, and waste reservoirs was connected with tubing and assembled outside the incubator. The pump (DK Infusek) was turned on until the air bubbles in the syringes and tubing were eliminated. The setup was then transferred to the incubator, and the pump was turned on with a volumetric flow rate of 30 μ L/h. The chips were incubated in a humidified incubator at 5% CO₂ and 37°C for 3 days, where fresh differentiation medium (Appendix 9.2.1, Table 9) was continuously pumped from the syringes through the respective perfusion channel of the chips into waste reservoirs via tubing sections in between. The conditioned media were collected each day and stored at -80°C.

3.3.5. Cell extraction of chips

After 3 days, the cells were extracted. The hydrogel was treated with 2 mg/mL of collagenase II (Worthington Biochemical) for 30 min inside an incubator. The collagenase step was performed twice and with strong resuspending to ensure complete cell removal from the chips. Cells from two or three chips were pooled together in one tube using proliferation medium. The tubes were then centrifuged for 5 min at 300 g. The medium was removed, and the cells were ready for RNA isolation.

3.3.6. RNA isolation and cDNA synthesis

Total RNA was extracted from the chips using the NucleoSpin RNA Plant kit (Macherey-Nagel) following the manufacturer's instructions. The elution step was performed with 30 μ L of RNase-Free water. The concentration of RNA was determined using a spectrophotometer (NanoDrop ND1000). The A260/A280 and A260/A230 values for all RNA samples were > 1.37 and > 0.41.

cDNA was synthesized using 40 ng of RNA and the iScript™ cDNA Synthesis Kit (Bio-Rad Laboratories). Each sample received 4.0 μ L of iScript™ Reaction Mix and 1.0 μ L iScript™ Reverse Transcriptase. The reaction volume was adjusted to 20 μ L with nuclease-free water. After centrifuging, all samples were incubated in the Arktik™ Thermal Cycler (Thermo Fisher Scientific) at 25°C for 5 min, followed by 42°C for 30 min, and 85°C for 5 min.

3.3.7. RT-qPCR

All cDNA samples were diluted to a concentration of 0.25 ng/ μ L with nuclease-free water. In the respective duplicate columns of the 384-well plate (Appendix 9.2.2, Table 11), 2.0 μ L of diluted cDNA was added. Additionally, duplicate wells containing 2.0 μ L of nuclease-free water were used as no-RT controls.

In a set of 36 primers (Appendix 9.2.2, Table 10) was for each primer (Sigma-Aldrich) a total volume of 0.64 μ L forward and reverse primers, 32 μ L of SensiMix™ SYBR & Fluorescein (Bioline), and 14.72 μ L nuclease-free water used as primer mix. A volume of 6.0 μ L primer mix was added to the respective row of the 384-well plate (Appendix 9.2.2, Table 11). The plate was sealed with adhesive foil to prevent evaporation. After spinning the plate with the Centrifuge 5810R (Eppendorf) for 3 min at 2000 rcf, the plate was loaded into the CFX384™ Touch Real-Time PCR (Bio-Rad Laboratories). The samples were heated at 95°C for 10 min to denature the cDNA, followed by 40 cycles of denaturation at 95°C for 10 sec, annealing at 60°C for 15 sec, and extension at 72°C for 15 sec. The housekeeping gene 18S was used for normalization. Relative gene expression was determined using the comparative threshold cycle ($2^{-\Delta CT}$) method, with normalization to the housekeeping gene. Expression values around 40 cycles were not considered.

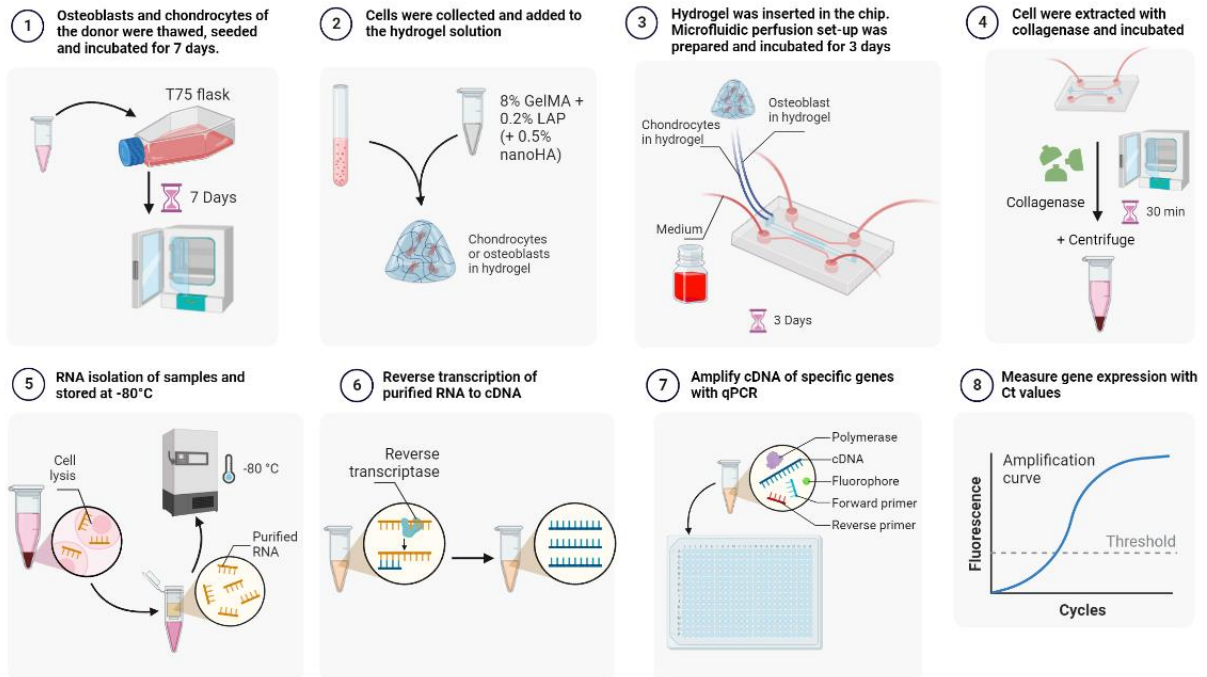


Figure 9. Schematic flowchart illustrating culturing of osteoarthritis-on-chip-model, as described in section 3.3 of the materials and methods. The flowchart is divided into eight important steps. (1) The cells were thawed, seeded, and incubated for seven days. (2) Cell collection and addition to GelMA solution. After the incubation period, the cells were collected and added to the GelMA solution. Osteoblasts were combined with hydrogel containing nanoHA, while chondrocytes were added to hydrogel without nanoHA. (3) The hydrogel containing the cells was added to the compartments on each chip. The chips, along with the perfusion setup, were incubated for three days. (4) The cells were extracted from the hydrogel using collagenase II after a 30-minute incubation period. (5) The RNA was isolated from the cells and stored or used for further analyses. (6) The isolated RNA was synthesized into complementary DNA (cDNA). (7) RT-qPCR analyses of specific genes. The synthesized cDNA was subjected to real-time quantitative polymerase chain reaction (RT-qPCR) to analyze the expression of specific genes, as listed in Table 10 of Appendix 9.9.2. (8) The threshold value of each gene was determined through qPCR analyses and evaluated across different donors. The figure was created with the Biorender app.

4. Results of the holder

This section presents the design process of the holder, incorporating the define, measure, analyze, and design step. Detailed information about the specifications, concept development, material choices, and production drawings can be found in the Appendix section 9.1.

4.1. Define phase of the holder

The holder comprises of several components: the syringe pump, the chip-holder, the waste tube holder, the baseplate, and the chips. The SPLab10 (DK Infusek) syringe pump, previously utilized by the AOT group, was selected for this project due to its compact size and lightweight nature compared to other options. It can contain up to ten syringes (see Figure 28B in Appendix 9.1.1). The second part, the chip-holder, serves the purpose of positioning the multiple organs-on-chips during transportation, such as to and from the microscope. The third part, the waste tube holder allows for the collection of conditioned media from each individual chip, enabling precise analyses of cell secretion. However, the analysis of cell secretion is beyond the scope of this research. To facilitate transportation and keeping all components together, a baseplate is essential. Lastly, the chips will be positioned inside the chip-holder. A pre-existing protocol for fabricating the double compartment chips was used (section 3.1 of materials and methods). Consequently, only the chip-holder, waste tube holder, and baseplate needed to be designed with the Six Sigma methodology (see Figure 10).

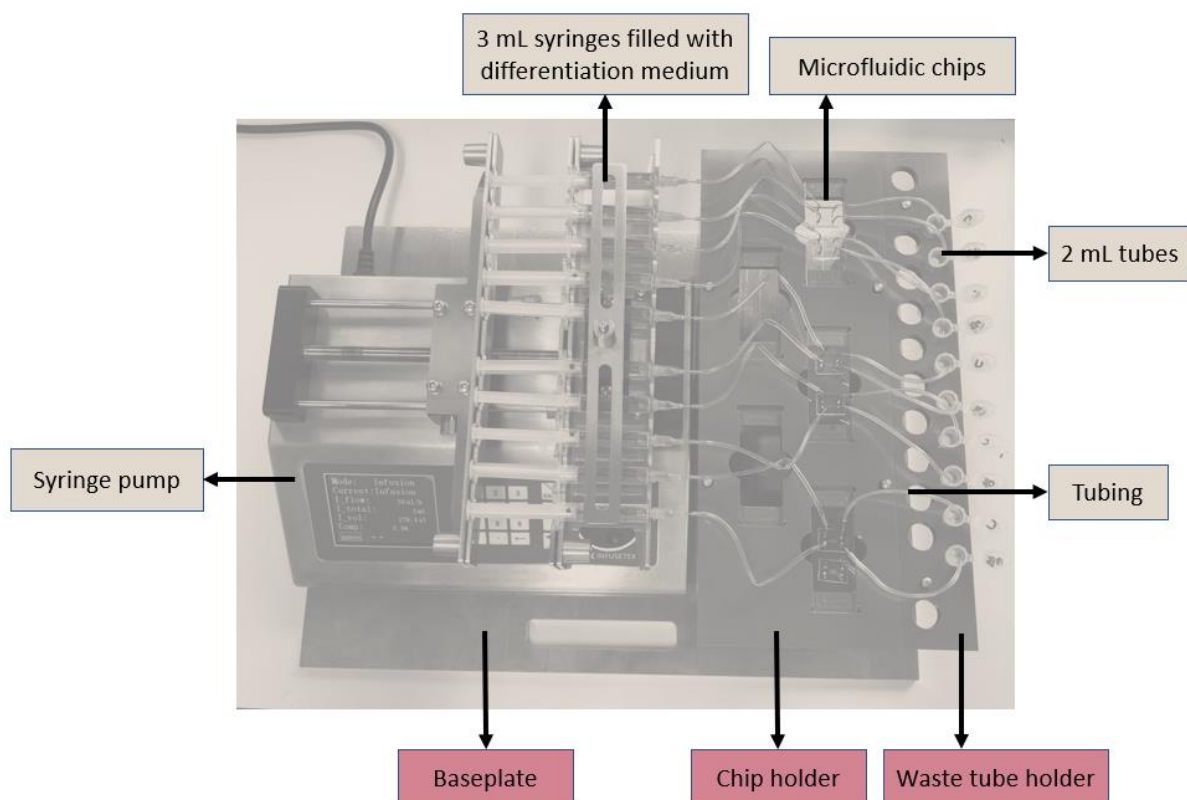


Figure 10. Components of the holder used in the project. The chosen syringe pump is the SPLab10 (DK Infusek), capable of ten syringes. Its dimensions are 288 x 280 x 175 mm (length x width x height), and it weighs 5.78 kg. Each syringe is filled with 3 mL of differentiation medium. Tubing connects the syringes to the osteoarthritis-on-a-chip, which are bonded to a microscope slide. Dimensions of the microscope slides are 76 x 26 x 1 mm (length x width x height). The chips can be inserted into the chip-holder, while tubes are placed inside the waste tube holder. The tubing is connected to chips for collecting conditioned media. All components are positioned on top of the baseplate. The pink components in the figure represent the parts that needed to be designed, while the other components already exist in the laboratory. Only the tubing required minor adjustments.

4.2. Measure phase of the holder

Based on objectives outlined in section 2.1.2. and considering the dimensions of the pump and incubator, a list of requirements has been obtained. This list was further extended through discussions with the users to ensure its completeness. The requirements primarily focus on the individual components for production, including the chip-holder, waste tube holder, baseplate, and chips. The syringe pump itself was not included in the requirements as it was not directly involved in the design process. Only the dimensions of the pump were considered when designing the baseplate. The complete list of requirements is presented in Table 1, where the MoSCoW method was used to prioritize the requirements based on their importance. The “M” (Must have) refers to essential requirements, while the “S” (Should have) relies on important requirements with significant values. The “C” (Could have) category includes requirements that provide additional value but were of less priority. Finally, the “W” (Will not have) was not included as the list was already extensive [38].

Table 1. List of requirements for organ-on-a-chip holder with four categories; the chip-holder, waste tube holder, baseplate, and chips. All requirements were rated on importance with the MoSCoW method.

	Requirements	Reasoning	MoSCoW
Chip-holder			
1.1	The chip-holder shall provide five microscope slide places.	The maximum capacity of the syringe pump is ten, and each chip requires two inlets connected to the syringe. Five fully supplied chips can be perfused with the use of a splitter.	M
1.2	The chip-holder shall stabilize the microscope slides.	The holder should prevent bumping and maintain the balance of the liquid inside the chips.	M
1.3	The microscope slides shall be pulled out from the chip-holder.	The slides should be able to be manually removed while maintaining the balance of the chips.	M
1.4	The chip-holder shall fit under the microscope.	The chip-holder should easily be transportable to the microscope for observation of the cells.	S
1.5	The chip-holder shall contain openings to see the chips under the microscope.	The holes should align directly beneath the chips to avoid the need for additional replacements.	M
1.6	The chip-holder shall easily be disconnected from the baseplate.	Detaching the chip-holder makes it more portable.	M
1.7	The height of the chip-holder shall be lower than the height of syringe pump.	Having a small height difference improves the perfusion flow.	S
Waste tube holder			
2.1	The waste tube holder shall easily be disconnected from the baseplate.	The collector should be removable for investigating the conditioned media or replacing reservoirs.	S
2.2	The waste tube holder shall be separate and portable from the chip-holder.	The holder should be independently relocatable.	S
2.3	The waste tube holder shall fixate the tubes.	The reservoirs should be secured by the collector to prevent spilling.	S
2.4	The waste tube holder shall consist of a minimum of two different hole sizes.	Providing options for tube size allows flexibility based on research duration.	C
2.5	The reservoirs shall easily be removed from the waste tube holder.	Easy removal of reservoirs enables investigation after their removal from the collector.	M
Baseplate			
3.1	The baseplate shall fit inside the incubator.	The total holder must not exceed dimensions of 450 mm in length and width to fit in the incubator.	M
3.2	The height of the total holder, including the baseplate, shall be lower than 185 mm.	The overall height should not exceed 185 mm to fit within the incubator.	M
3.3	The chip-holder and waste tube holder shall be detachable from the baseplate.	Detachability allows for separate investigation or transportation of individual components.	S

3.4	The baseplate shall be able to carry the weight of the different parts.	The baseplate should have sufficient stiffness to prevent deformation caused by the weight of the equipment.	M
3.5	The strength of the baseplate shall be able to carry the weight of the different parts.	The baseplate should have sufficient strength to prevent overloading and deformation.	M
3.6	The baseplate shall be transportable.	The ability to move the holder over short distances, from incubator to workspace, is desirable.	S
3.7	The baseplate shall contain a minimum of three handgrips for transportation.	Handgrips facilitate tilting and transportation of the baseplate.	C
3.8	Everything shall be connected outside the incubator, except for the electrical pluck from the pump.	Connecting all components outside the incubator, except the pump's electrical plug, prevents prolonged incubator exposure and interference with incubator settings.	M
Chips			
4.1	The chips shall only be placed on top of the microscope slides (76 x 26 mm).	The holes fit exactly for the microscope slide dimensions.	M
4.2	A maximum of two chips shall be placed on one microscope slide.	Placing more chips would limit space for tubing and increase the risk of crosstalk.	C
4.3	The chips shall be placed above the holes from the chip-holder.	Corresponding holes on the chip-holder allow for easy investigation of the chips.	M
4.4	The chips shall be connected to the syringes with tubing.	The chips need to be connected to the syringes located at the pump.	M
4.5	The chips shall be connected to the waste tube holder with tubing.	The chips should be connected to the reservoirs located at the waste tube holder.	M
4.6	The tubing should be less crowded.	Proper placement of tubing is required to minimize crowding and prevent potential crosstalk, which impacts the flow in the system.	S

4.3. Analyze phase of the holder

After considering the requirements listed in Table 1, we produced different concepts for the chip-holder. Before making any decisions, we needed to determine the pumping system direction and chip orientation. A detailed justification for these choices can be found in Appendix 9.1.1. In summary, the infusion system was more favorable due to its ease of collecting conditioned media, aligning with the goals set by the users. Regarding chip orientation, a horizontal chip placement with vertical microscope slide was determined to be optimal, as it reduced the tubing crowding. This consideration was also reflected in the three designed concepts (Appendix 9.1.3, Table 4), with concept 1 being the preferred option. Concept 1 allowed for the original chip arrangement and accommodated up to ten chips without causing tubing congestion.

Moving on to the waste tube holder, two concepts were developed and evaluated (Appendix 9.1.3, Table 5). It was concluded that concept 2 offered easier production and fixation (Figure 12). However, concept 2 had the limitation of not being able to stand independently inside a fume hood. To address this issue, a tubing rack can be used to provide stability.

Figure 11 illustrates the assembly of the selected chip-holder and waste tube holder. The waste tube holder was connected to the support rib using two triangles, which were secured with four screws. The top plates were interconnected to their supports via pins, enabling the plates to be relocated if needed.

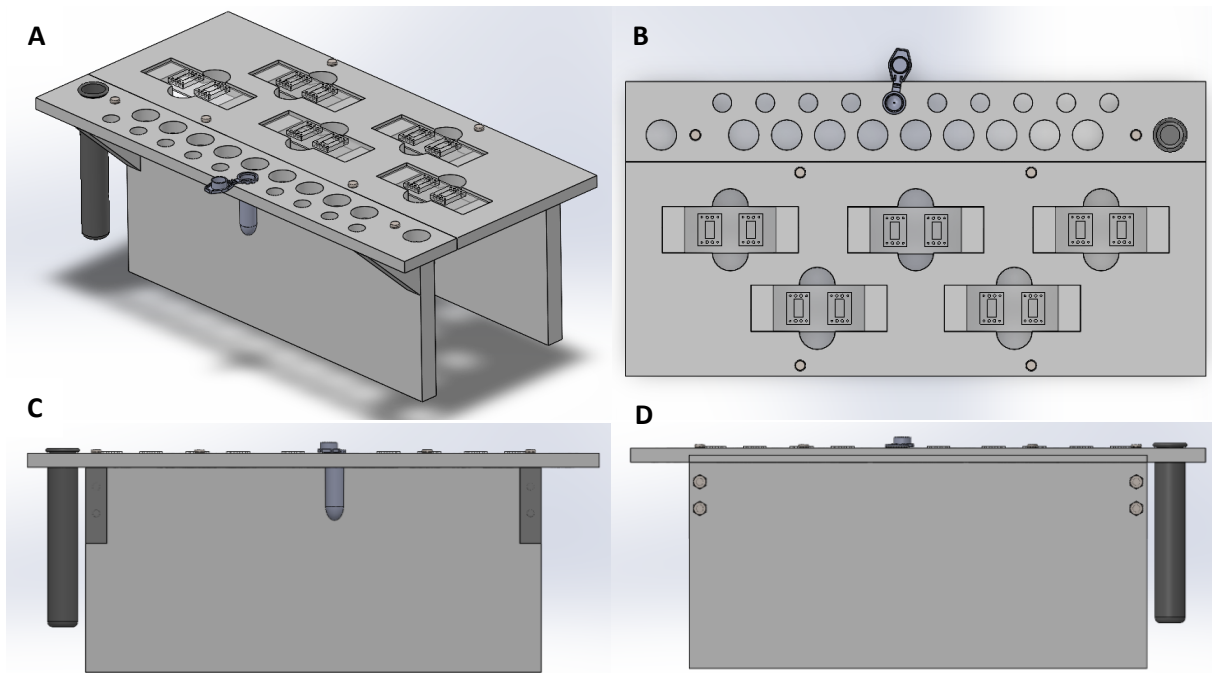


Figure 11. Assembly of selected chip-holder and waste tube holder, created with SolidWorks. After detailed consideration, concept 1 (Table 4) was chosen as the optimal chip-holder design, while concept 2 (Table 5) was selected for the waste tube holder. Additional components, such as the 2 mL and 15 mL tubes and the microfluidic devices, were added to the assembly. The figure provides an isometric view (A), top view (B), side view (C), and cross-section view (D). The cross-section view shows the screw connection of the triangles to the support rib.

The next step involves the design of the baseplate, taking into consideration the dimensions of the chip-holder, waste tube holder (Figure 11), and pump. The baseplate design was intentionally kept simple. Only the handgrips were variable in terms of length, width, location, and quantity. As a result, a simple single concept was developed, as depicted in Figure 12. It incorporates the placement of the support ribs from the chip-holder.

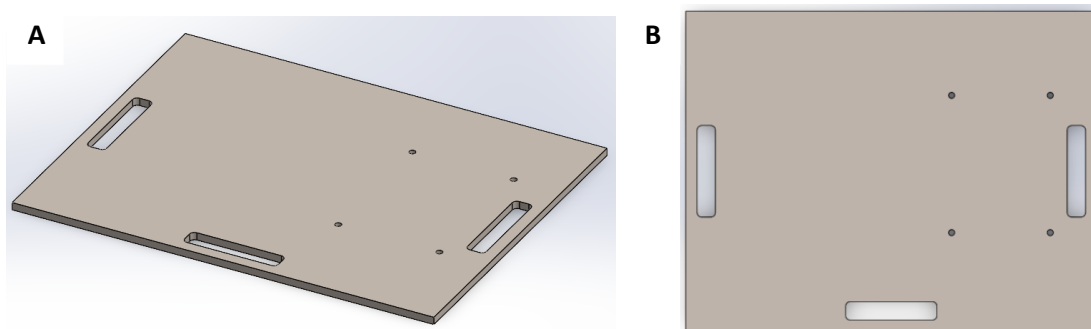


Figure 12. Baseplate design created in SolidWorks. The location of the support ribs of the chip-holder were already positioned in the design. An isometric view (A) and a top view (B) of the baseplate.

To achieve a comprehensive design, the best concepts were integrated into a complex assembly using SolidWorks. This included extra features, such as a pumping system sketch, 3 mL syringes, chips, and 2 mL tubes, and 15 mL tubes. The complete assembly of the holder, including all its components, can be seen in Figure 13. Additionally, a detailed drawing of the assembly was produced (Figure 14), illustrating all components of the holder with a Bill-of-Material (BOM) list.

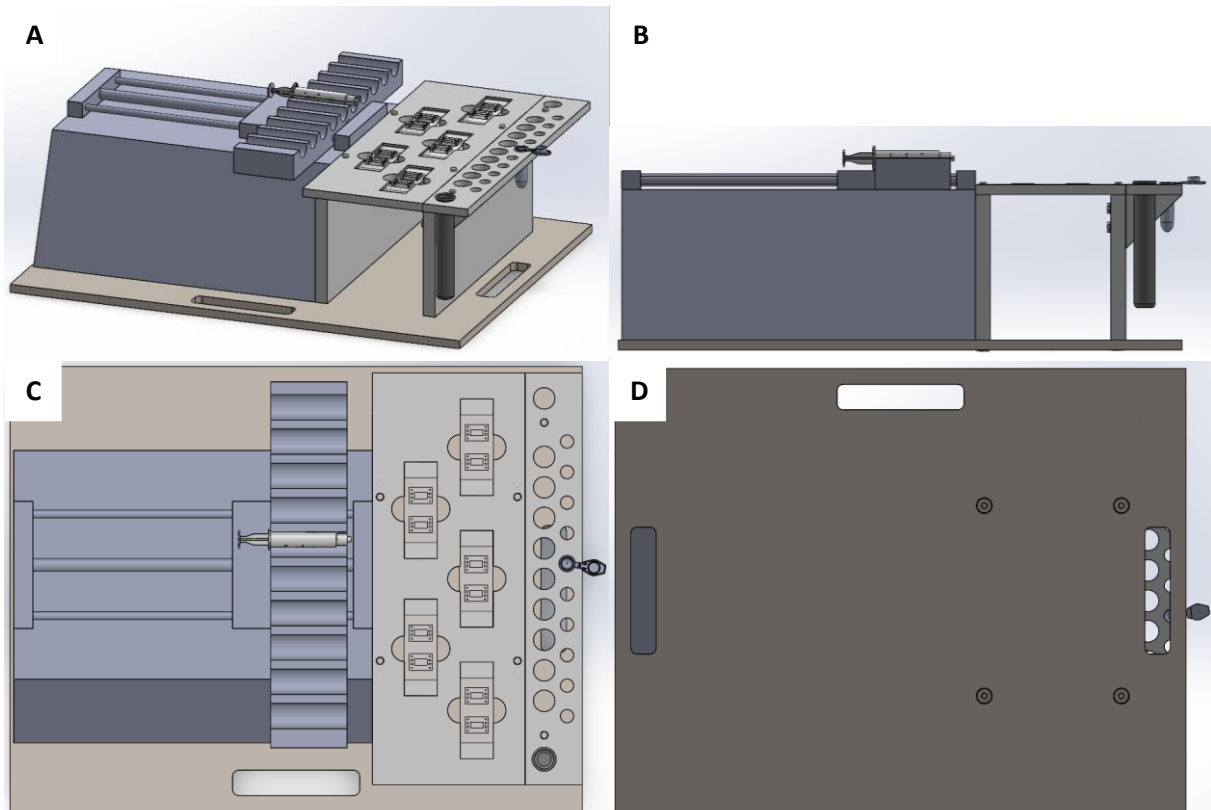


Figure 13. Total assembly of the holder including every part produced in SolidWorks, providing isometric (A), side (B), top (C), and bottom (D) view.

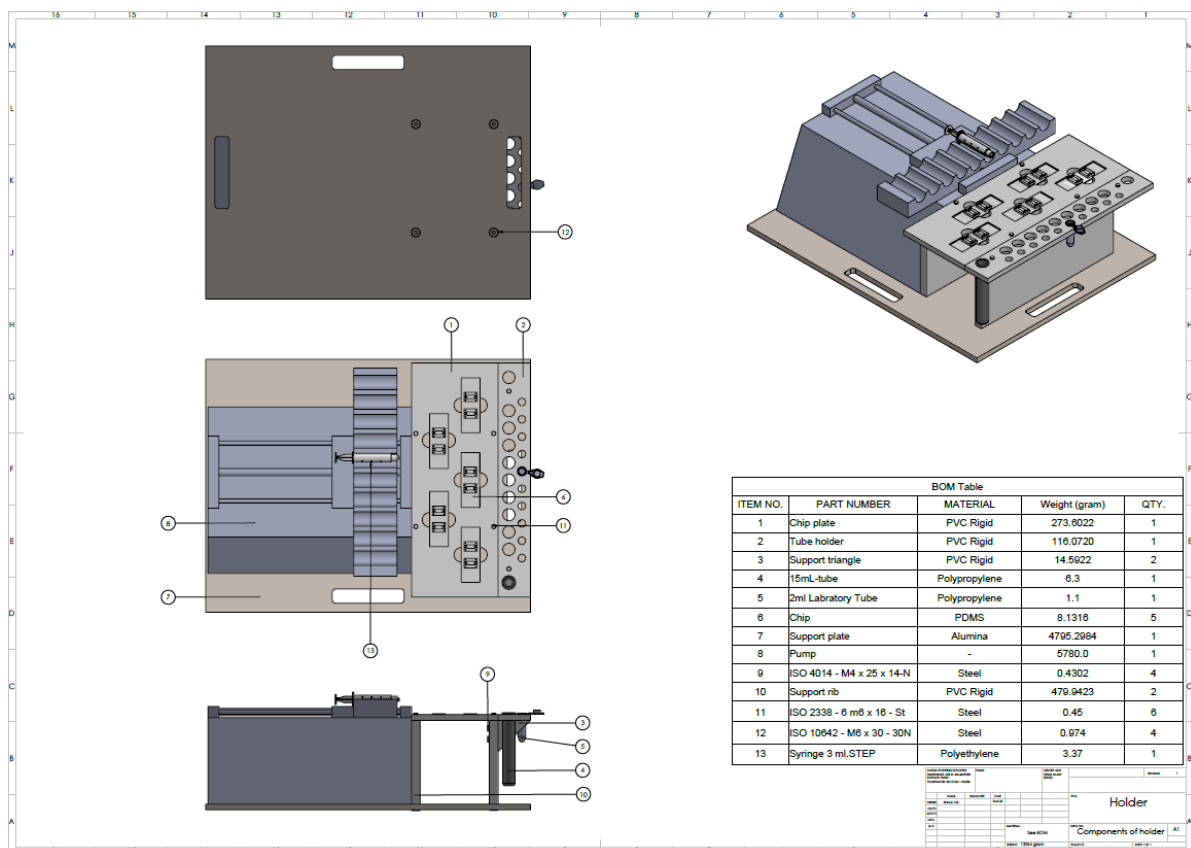


Figure 14. Drawing of assembly obtained using SolidWorks. The drawing illustrates all components of the holder along with their materials, weights, and quantities. The balloons in the drawing correspond to the item numbers in the Bill-Of-Material (BOM) table.

4.4. Design phase of the holder

4.4.1. Design of components

The design of the components was translated into production drawings for workshop use, as shown in Appendix 9.1.5. The manufacturing process involved the fabrication of the parts, including the support ribs (Figure 15A), chip-plate and waste tube plate (Figure 15B), triangles (Figure 15C), and baseplate. All components were made from grey polyvinyl chloride (PVC), except the baseplate which was made from aluminum. Detailed information regarding the material choices can be found in Appendix 9.1.4.

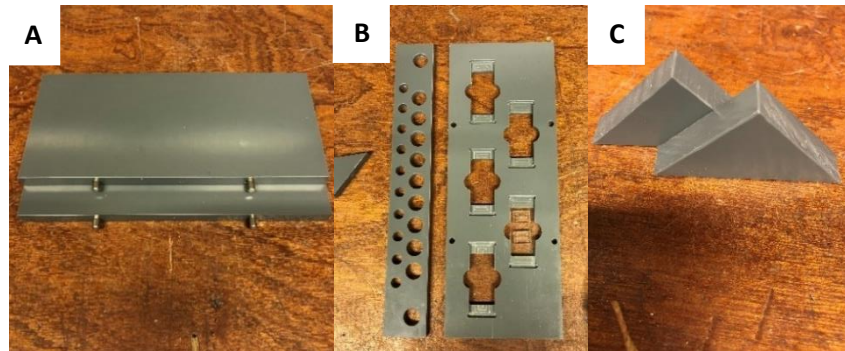


Figure 15. Individual components created within the University of Twente workshop. (A) Two support ribs with pins for connection to the chip-plate. (B) The waste tube plate on the left side, and the chip-plate on the right side. (C) Two triangles provided for connecting the tube-plate to the support rib of the chip-holder.

4.4.2. Product

Moving on to the final product, as illustrated in Figure 16 and Appendix 9.1.6 (Figure 35). Figure 16A and 16B provide a visual presentation of the completed holder produced in the workshop. In Figure 16C, we can observe the complete setup of the holder within the laboratory environment, positioned outside the incubator. This includes the syringe pump, medium-filled syringes, chips containing cells, 2 mL waste reservoirs, and interconnected tubing. Figure 16D illustrates a full setup of the holder positioned inside the incubator as used for three days in this research.

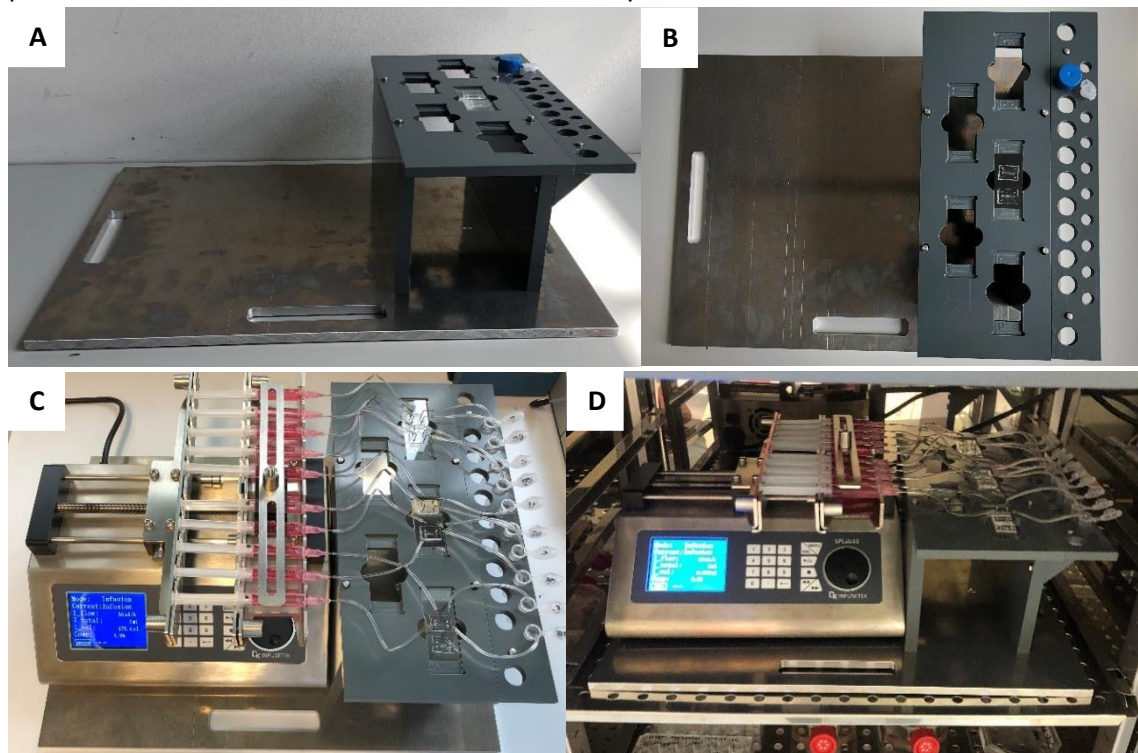


Figure 16. Assembled product of the holder. Completed holder produced in the workshop, with front (A) and top view (B). Complete setup of the holder used for the experiments, including outside (C) and inside (D) the incubator.

The final product can obtain multiple functions as listed in Table 2. These functions support the successful implementation of osteoarthritis-on-chip experiments. It had proved to be an efficient and controlled holder for studying the disease.

Table 2. Functions of product.

Functions	Product specifications
Capacity	The chip-holder contains up to five microscope slides, allowing for ten chips to be perfused by using a splitter. The 2 mL tube has a maximum capacity of ten, and the 15 mL tubes can hold eleven.
Chip stability	The holder securely positions organs-on-chips during experiments and transportation.
Collection of conditioned media	The waste tube holder component allows for the collection of conditioned media produced by the cells. This facilitates further analyses of cell secretion.
Dimensions	The holder has specific dimensions of 350 mm x 450 mm x 175 mm (length x width x height) to have sufficient space inside the incubator.
Experimental control	The holder provides a controlled environment for osteoarthritis-on-chip experiments, allowing researchers to adapt experimental parameters.
Facilitate transportation	The design of the holder allows for transportation of organs-on-chips over various locations.
Fluid management	The holder enables controlled fluid flow and perfusion through the chips.
Mass	The estimated total mass of the product is approximately 12 kg, as calculated with SolidWorks.
Material considerations	The choice of materials, PVC for the plates and aluminum for the baseplate, ensures durability and suitability.
Modular design	The holder is designed to be modular, allowing easy interchangeability of components. The top-plates of the chip and waste tube holder can be easily taken out.

The designed holder can be translated from the academic context to the industrial design (Appendix 9.1.8, Table 7). In the industrial design settings, the requirements and considerations differ as it needs to be designed for continuous and robust operations, with multiple users and potential 24/7 usage. Upscaling the syringes beyond the current maximum capacity may be necessary. Also, automated production processes are preferred to ensure efficiency and consistency. Integration of smart features and connectivity, such as sensors for monitoring parameters, may become relevant in the industrial setting. Moreover, material optimization plays a crucial role in feasibility of production as the research domain of the holder may be extended.

5. Results of the osteoarthritis-on-chip model

This section includes the results of biological experiments. Starting with the observations of the cells, followed by RNA nanodrop values, and RT-qPCR results. The perspectives of the results will be analyzed regarding literature research.

5.1. Observations

Two donors, one male (D2/103) and one postmenopausal female (D1/74), were analyzed in this study. The characteristics of the cells in culture and on microfluidic chips are presented in Figure 17. Two additional donors were excluded from the study due to pre-existing infections.

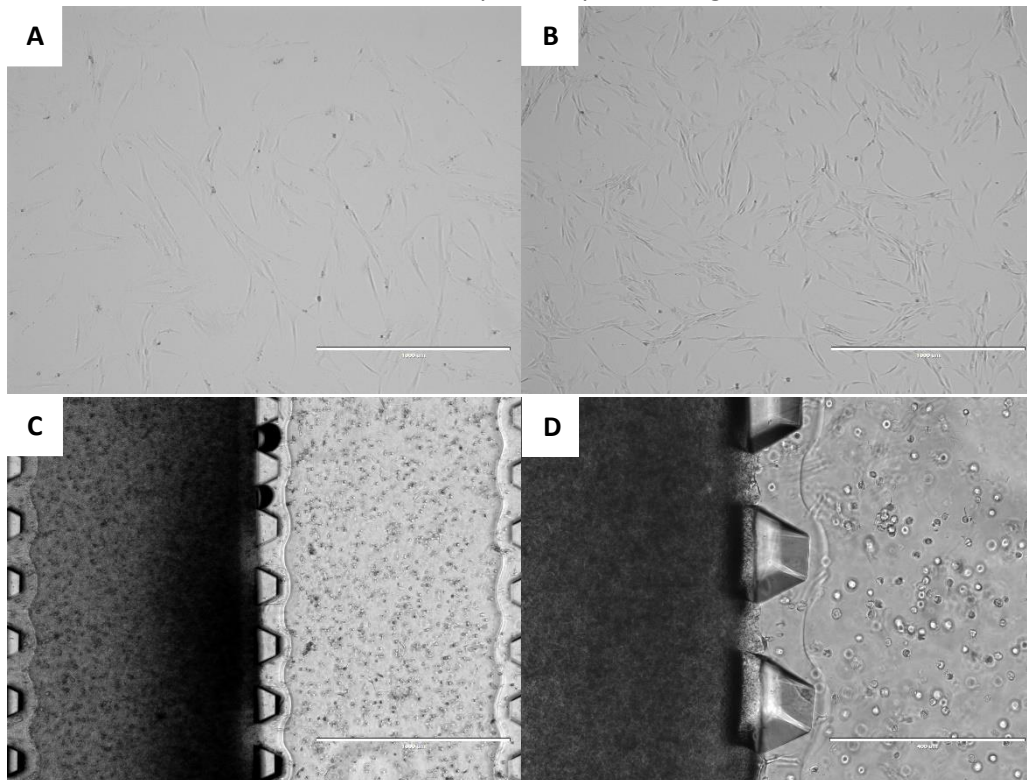


Figure 17. Osteoblast and chondrocyte cells. (A) Osteoblasts of donor 1 at day 7 after seeding (magnification 4x). (B) Chondrocytes of donor 74 at day 7 after seeding (magnification 4x). (C) Microfluidic chips filled with osteoblasts in a mineralized hydrogel network in the dark compartment (left), and chondrocytes in hydrogel networks on the light compartment (right). The picture was taken on day 3 of perfusion (magnification 4x). (D) Close-up view of the boundary between the two hydrogel layers (magnification 10x). Scale bars: A, B and C: 1000 μm and D: 400 μm .

5.2. RNA isolation values

Total RNA was isolated from the microfluidic chips. Two or three chips were pooled together to obtain two tubes for each donor. The amount of RNA was determined using nanodrop measurement, and the results are presented in Table 3. RNA values fluctuated between 4.0 $\text{ng}/\mu\text{L}$ and 9.2 $\text{ng}/\mu\text{L}$.

Table 3. Nanodrop measurement of RNA from two donors. The amount of RNA was measured along with 260/280 and 260/230 (RNA purity). D1/74 represents a female donor, and D2/103 represents a male donor.

	D1/74 Tube 1	D1/74 Tube 2	D2/103 Tube 1	D2/103 Tube 2
Amount of RNA ($\text{ng}/\mu\text{L}$)	9.2	5.8	4.0	8.7
260/280	1.91	1.37	2.21	1.64
260/230	0.81	0.55	0.41	0.57

5.3. Gene expression

The relative gene expression was determined by normalizing the CT values to the housekeeping gene 18S. However, due to limited data available, statistical analyses could not be conducted. The average CT values for the housekeeping gene were 25.34 and 26.34 for D1/74, 25.74 and 26.80 for D2/103. Amplification of single product in each reaction was confirmed by melting curve analyses.

A primer panel consisting of protein coding genes and genes (36 different primers) was categorized into matrix remodeling, receptor, WNT pathway, growth factor, inflammatory cytokines, osteoclast, osteoblast/chondrocyte, and toll-like receptor. These primers were selected based on osteoblast and chondrocyte activities and the review by Klein et al.[24] regarding sex differences in innate immune responses in adults.

The results are in categories presented in figures 18 and 19. Overall, it is evident that D1/74 (female) expresses a greater number of genes among these genes analyzed compared to D2/103 (male). ESR1, IL-1 β , MMP9, and RANKL were expressed by D1/74 but not by D2/103. Conversely, only SP7 and TLR4 were expressed by D2/103 and not by D1/74 (Figure 20). Seventeen primers were expressed by both donors, while eleven primers were not expressed.

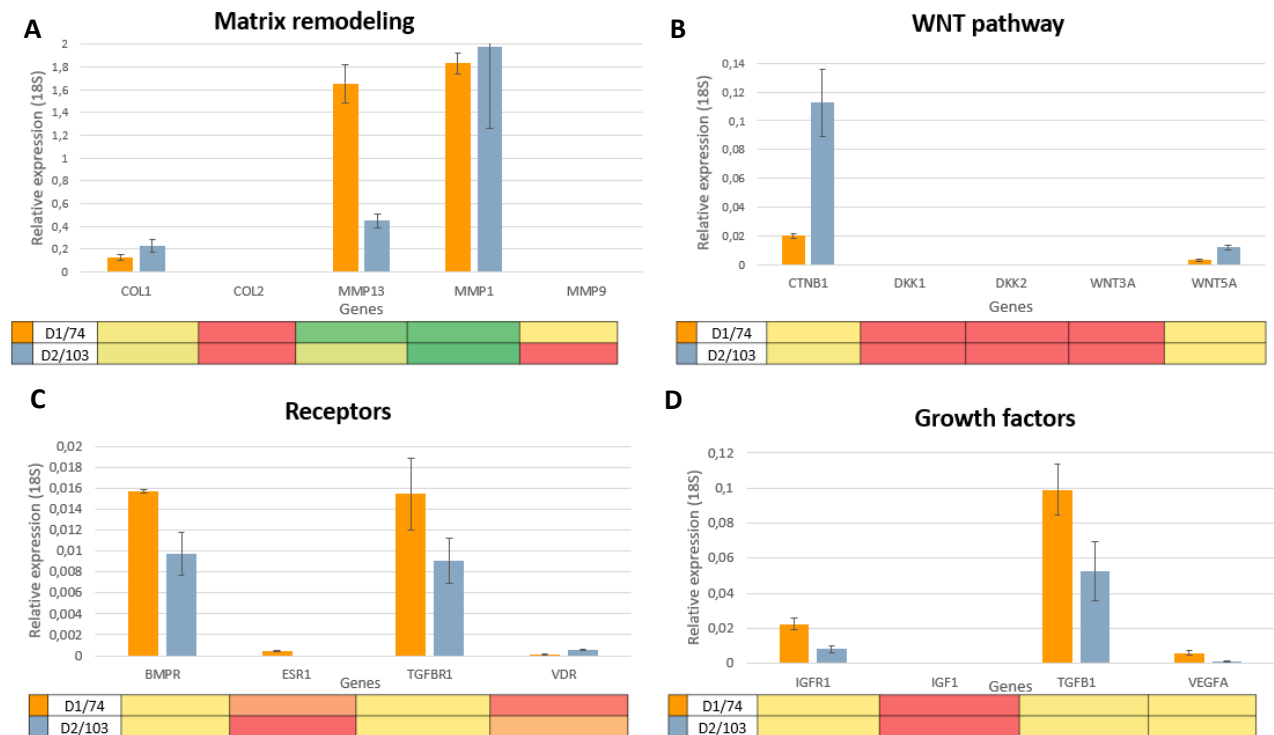


Figure 18. The relative gene expression profiles of D1/74 (a female donor represented in orange) and D2/103 (a male donor represented in blue). The expression of (A) matrix remodeling (COL1, COL2, MMP13, MMP1, MMP9), (B) WNT pathway (CTNB1, DKK1, DKK2, WNT3A, WNT5A), (C) receptors (BMPR, ESR1, TGFB1, VDR) and (D) growth factors (IGFR1, IGF1, TGFB1, VEGFA). The graphs present the $2^{-\Delta CT}$ values, which have been normalized using the housekeeping gene 18S. Mean values \pm standard deviation (SD) is provided, with a sample size (N) of 1. Heat maps have been included to compare the expression of all genes, with green indicating high expression and red indicating no expression.

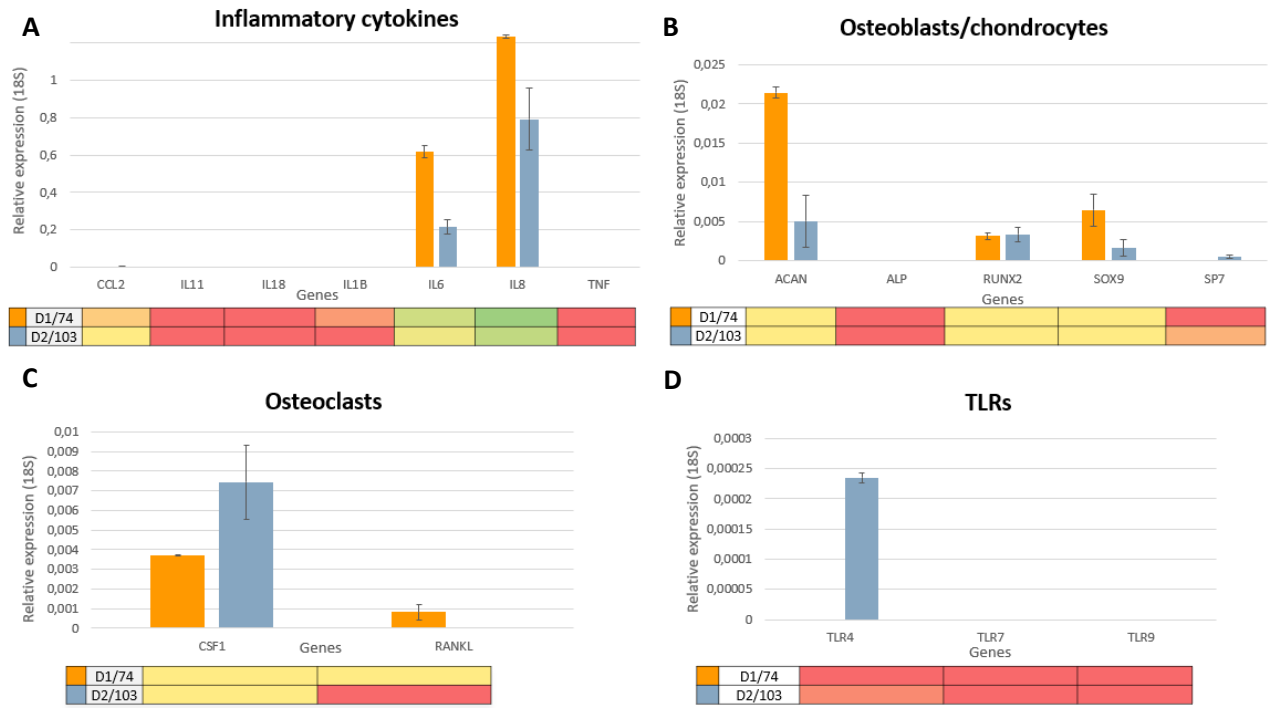


Figure 19. The relative gene expression profiles of D1/74 (a female donor represented in orange) and D2/103 (a male donor represented in blue). The expression of (A) inflammatory cytokines (CCL2, IL-11, IL-18, IL-1 β , IL-6, IL-8, TNF), (B) osteoblasts/chondrocytes (ACAN, ALP, RUNX2, SOX9, SP7), (C) osteoclasts (CSF1, RANKL), and (D) TLRs (TLR4, TLR7, TLR9). The graphs present the $2^{-\Delta CT}$ values, which have been normalized using the housekeeping gene 18S. Mean values \pm standard deviation (SD) is provided, with a sample size (N) of 1. Heat maps have been included to compare the expression of all genes, with green indicating high expression and red indicating no expression.

Differences in gene expression

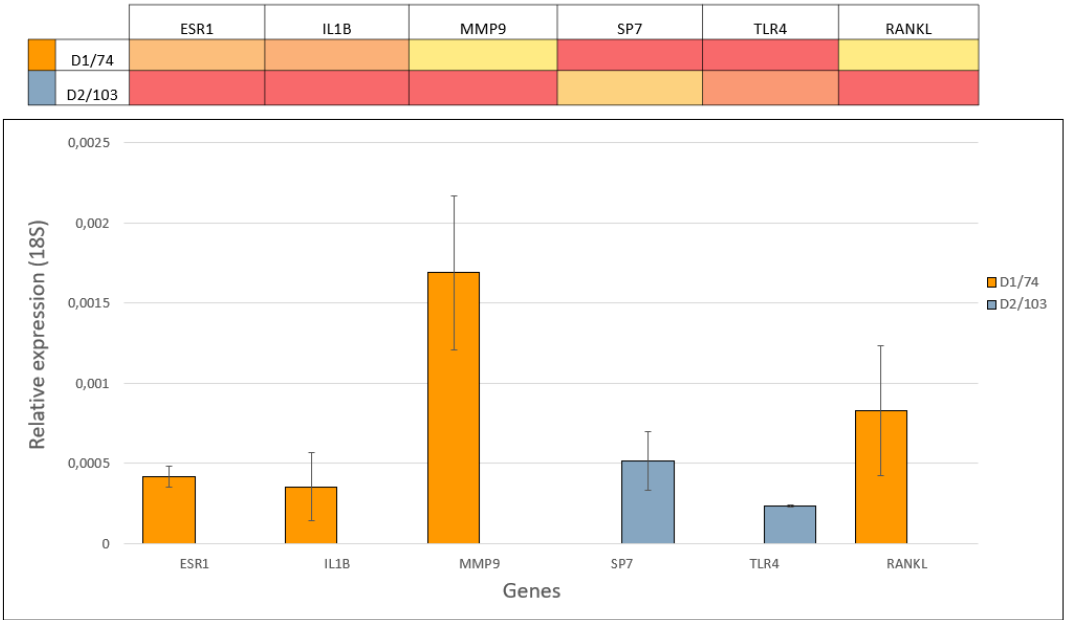


Figure 20. Differences in relative gene expression were examined between D1/74 (female donor represented in orange) and D2/103 (male donor represented in blue). The graphs represent the $2^{-\Delta CT}$ values, which were normalized using the housekeeping gene 18S. Mean values \pm standard deviation (SD), with a sample size (N) of 1. Notably, ESR1, IL-1 β , MMP9, and RANKL were expressed in D1/74 but not in D2/103. Conversely, SP7 and TLR4 were expressed in D2/103 and not in D1/74. Heat maps were included to compare the expression of all genes, with green indicating high expression and red indicating no expression.

5.4. Perspectives of results

The RT-qPCR results demonstrated the expression of various genes. Comparing our findings with the literature research in the introduction, we observed the expressions of MMP1, MMP13, TGF β , VEGF (Figure 3), IL-6, CCL2, and RUNX2, indicating the presence of OA. We expected to detect TNF- α (Figure 3), IGF, COL2, MMP 9, TLR7 and TLR9; however, these genes were not detected in our study. Only TLR4 showed a potential higher expression in males, while IL-1 β and IL-6 showed a potential higher expression in females. It is important to note that due to the limited sample size in our study (N=1), definitive conclusions cannot be drawn.

Contartese et al.[6] reviewed all existing preclinical studies regarding sex differences in OA and found a total of 426 samples *in vitro*, 458 mice's and 294 rats *in vivo*. However, conducting research with such extensive numbers in human patients' experiments is difficult. They suggested that subject groups with fewer than 20 patients can be considered as small. Insufficient sample sizes fail to provide adequate statistical evidence for sex differences because other factors, such as age and genetics, influences the experimental outcomes. Therefore, an extensive number of patients must be examined before conclusions can be drawn [6]. Even replicating our research with 20 patients would be time-consuming. However, to determine the specific number needed for the research, calculations can be performed. This considers factors such as the expected effect size, statistical power (typically 0.8), significance level (normally 0.05), and variability of the data [39]. The exact number of samples needed to obtain conclusions regarding sex-specific differences can be determined in further research.

To address the variability of the results, we can have a look at the levels of markers in human synovial fluids using the multiplex ELISA method. From a study involving 81 males and 115 female participants were the results graphically represented in Figure 21 [40]. The extensive variability observed for each marker suggests that decreasing the number of patients could heavily influence the reliability of the mean value. Therefore, it is advisable to include a larger number of patients to account for the fluctuations within the same sex group. Although a different method was used in this study, the same phenomenon may apply.

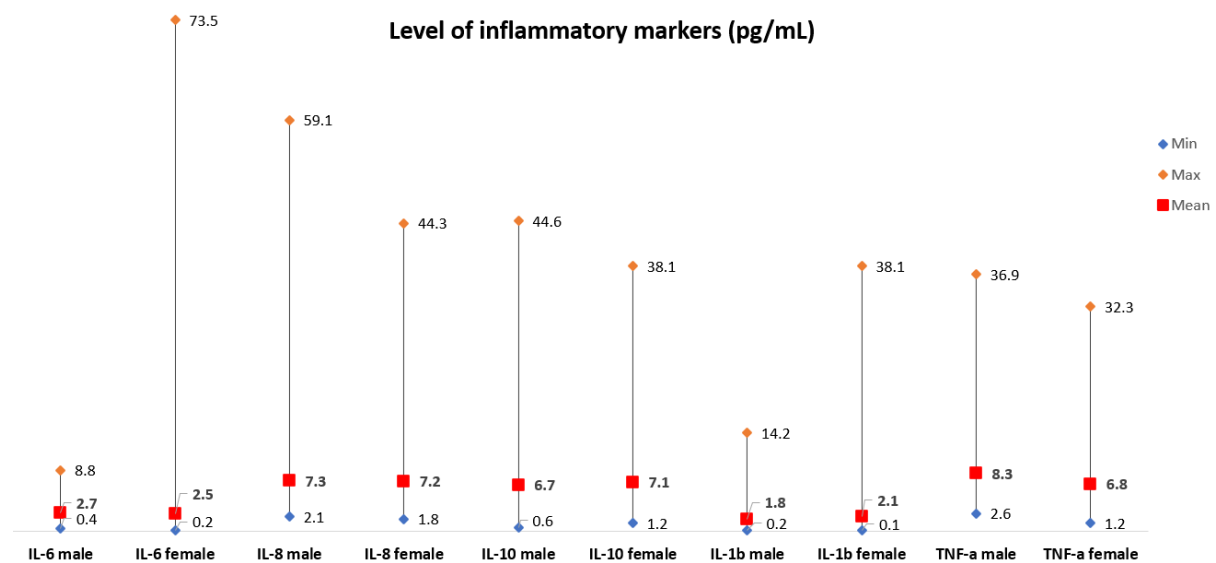


Figure 21. Perruccio's research involved the measurement of inflammatory cytokine levels (IL-6, IL-8, IL-10, IL-1 β , and TNF- α) using the multiplex ELISA method. The data obtained in the report were used to construct a graph, which demonstrates a considerable range of variations within each gender category. It is crucial to consider the reliability of mean values as the number of patients decreases [40].

6. Discussion

Taken together, the data demonstrated the usability of the holder and microfluidic OA chips for gene expression analyses. In this section, we will discuss the design challenges of the holder system, explore potential enhancements, and outline future perspectives. Additionally, we will discuss the outcomes of the OA model experiments, along with challenges and future perspectives.

6.1. The holder system

As part of this study, we developed a holder system which can be used for perfusion system for microfluidic chips. Unfortunately, due to unforeseen circumstances, namely prior cell infection, it was not possible to conduct more than three experiments with this holder.

6.1.1. Verify phase of the holder

The final phase of the DMADV methodology involved verification of the product based on initial objectives and requirements. A detailed explanation can be found in Appendix 9.1.7. Only the objectives with potential improvements will be discussed.

One of the objectives of the holder was to provide independent accessibility of components. While it was possible to transport the chip-plate and tube-plate individually, we encountered difficulties when placing the tube-plate in an appropriate position in the fume hood. The tube-plate lacks stability, and the reservoirs did not fit into a standard 2 mL rack. As a solution, we used a 50 mL rack, but this aspect can be considered for an innovative design.

Another aim was to enable long-term utilization of the holder. In this research, the holder was used for three experiments, and determining its exact lifespan is challenging. There should be no limitations with the materials (Appendix 9.1.4.), except for potential restrictions of pump humidity percentage of <80%. In the product description of Nuair incubator type NU-5700, it was stated that the relative humidity inside the incubator was 95%. The impact of higher humidity conditions on the pump remains unknown. So far, we have not observed any limitation with the pump, but this should be considered when working with the setup inside the incubator.

Based on our experience with the holder, some requirements as listed in Table 1 (orange ones in revision list of Appendix 9.1.7, Table 6) can be improved. It was possible to observe the cells on the holder under a microscope but focusing on the cells was challenging due to the relatively thick plate. To reduce the distance, a thinner plate or deeper holes would be preferable. Additionally, we noticed that some reservoirs were relatively tight inside the holes due to PVC deformation. This aspect should have been paid more attention to in the fabrication process. Furthermore, the estimated total weight of the holder is 12 kg, primarily caused by pump (5.78 kg) and the aluminum baseplate. Alternative material can be considered for the baseplate that will be still strong enough to support the weight. Therefore, additional calculations regarding material deformation would be required. This was not necessary for the aluminum plate as it was extremely strong. Moreover, when removing the tube-plate to collect the conditioned media, we noticed that the tubing could lift the slides due to its stiffness. This issue could be avoided by creating a slit (Figure 22) or implementing a clicking mechanism, which prevents the chips from moving upwards. However, this modification would increase the complexity of production.

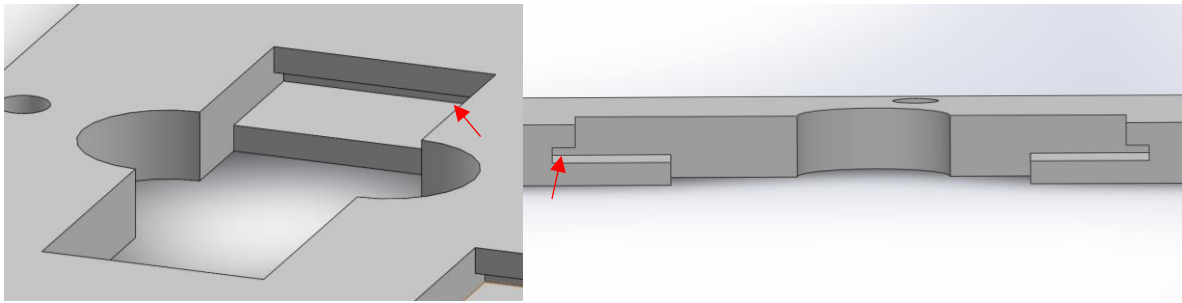


Figure 22. Possible modification of slit feature (addressed with red arrows) to the chip-plate to prevent the chips from moving up. Produced with SolidWorks. Isometric view (A) and cross-section view (B) of one chip location.

This design can easily be upscaled by implementing additional features. We noticed that sometimes the tubing was not connected properly, which could be avoided with sensors that can detect the flow of the medium. Upscaling the throughput of perfused chips is more challenging due to the pump's capacity. If a new pump with a higher syringe capacity is designed, the setup can be scaled up with an additional floor. The key considerations here would be the limited space inside the incubator and the maintenance of perfusion level in the system. An option with the current pump is the use of multiple splitters, although this would require larger volume syringes. However, the current pump is not capable of accurately perfusing small amounts ($30 \mu\text{L/h}$) with a 10 mL syringe. Using 3 mL volumes is not preferable when using more than two splitters as it would require frequent medium refilling and increasing the chance of air bubble formation.

6.1.2. Future perspectives of the holder

In the current design, PVC was chosen as a material for the chip-holder and waste tube holder. However, an alternative material would be polymethylmethacrylate (PMMA). PMMA is widely used in the design of platforms. It offers several advantages over PVC, including resistance to biological chemicals, optimal transparency, and low auto-fluorescence background [41]. When expanding the research domain with optical light courses, PMMA would be a preferable option.

In case we would like to increase the complexity of the holder, the system of Chao et al.[42] could be a valuable reference point. They used the system (Figure 23) for metabolizing drug molecules in human hepatocytes cultured under perfusion conditions.

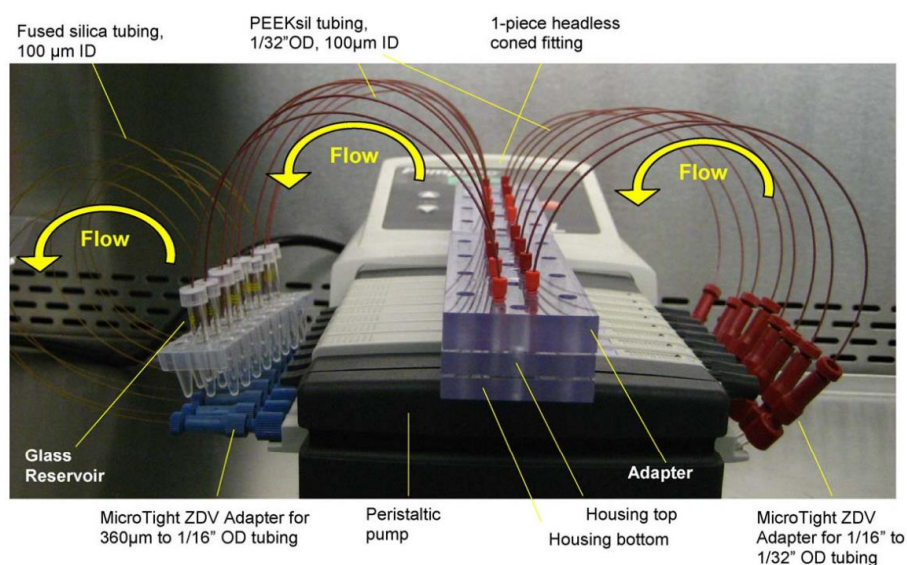


Figure 23. Complete setup of H μ REL prototype instrument. A peristaltic pump is used to generate culture medium flow. The housing includes four chips with cells [42].

In recent years, significant advancements have been made in the development of microfluidic platforms. Researchers have focused on designing microfluidic circuit boards, which integrate multiple components and functions onto a single platform. It enables precise control of volumes using sensors and detectors [43].

An example of such a platform is the mLSI MFBB (Figure 24), which has the capacity to screen up to 64 different conditions. This complex platform consists of clamps, an mLSI MFBB with 64 chambers, a fluidic circuit board, and an external interconnection block. The researchers expect that future developments will enable flexible integration of MFBBs in organs-on-chips and create body-on-a-chip systems. Therefore, this system looks very promising for applications in microfluidic cell culture [43]. However, before implementing this device in our specific research domain, further developments and adaptations need to be made. If cells can be extracted and gene expression analyses can be performed using this system, it would offer many benefits such as upscaling the number of conditions. The main challenge of implementing this system will probably be the costs.

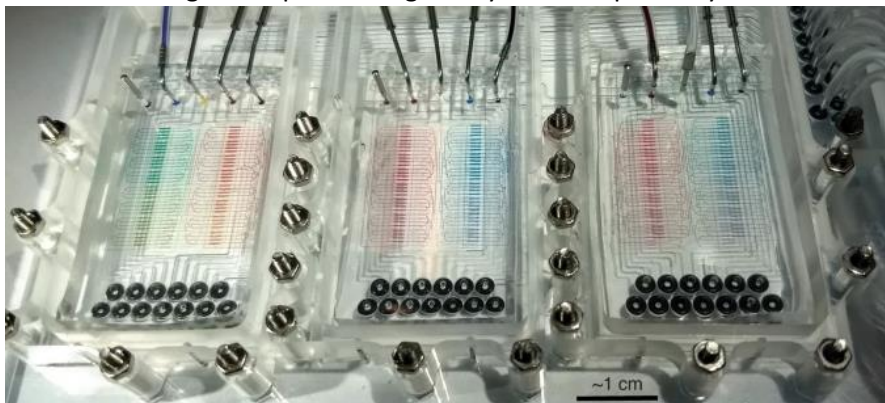


Figure 24. Assembled platform designed by University of Twente, consisting of three mLSI MFBBs filled with food coloring gradients [43].

6.2. The osteoarthritis-on-chip model

Our data showed a genetic profile of two chondrocyte and osteoblast donors under dynamical perfusion of pro-inflammatory cytokines for three days. There were some challenges in this research that will be discussed in this section. Also, future perspectives will be addressed.

6.2.1. Challenges

The organ-on-a-chip technology is currently not able to resemble a whole joint while OA is a multi-tissue system. Some components of the knee are articular cartilage, subchondral bone, synovial membrane, meniscus (in knee), and ligaments [33]. This research has only been focusing on osteoblasts and chondrocytes in a GelMA matrix. However, for an osteochondral interface, this might not be enough to establish the complex cooperations in OA resulting by lack of components such as nerves and blood vessels. They are normally invaded inside noncalcified cartilage. To better understand the disease, it is necessary to include more parameters and components by expanding the design of organ-on-a-chip [33, 36].

In vitro studies have the drawback of cell transformation or dedifferentiation which can influence the outcomes. Obtaining healthy human samples as a control group is difficult. In these experiments we used cells isolated from regions of diseased joints. Therefore, the status of healthiness of these cells can be questioned [6, 36]. Furthermore, an unexpected problem appeared in our research. Two chondrocyte donors were pre-infected, leading to a decreased number of investigated donors, namely two instead of four. This highlights the complexity of working with cells isolated from diseased joints.

Another challenge was that literature often compares healthy samples with OA samples without separation of gender. Only the research of Li et al.[44] showed heatmaps of differential expression genes between healthy and OA samples with respect to gender. Differences between healthy and OA samples could easily be obtained, while differences between male and female cells in OA were minimal [44].

Some intrinsic differences in gene expression between women and men expressed in chondrogenic progenitor cells were found in 2D and 3D culture by analyzing 372 patients, 238 women and 134 men. Interesting for our research was to observe significant differences in two cultural methods. A standardized level of Sox9, Col1 and Col2 expression in 3D culture was found to be higher in males than females (Figure 25A). While the ESR1 hormone receptor in 3D culture was higher in females than males [14]. It remains to be investigated how these expression patterns will differ when using the osteoarthritis-on-chip.

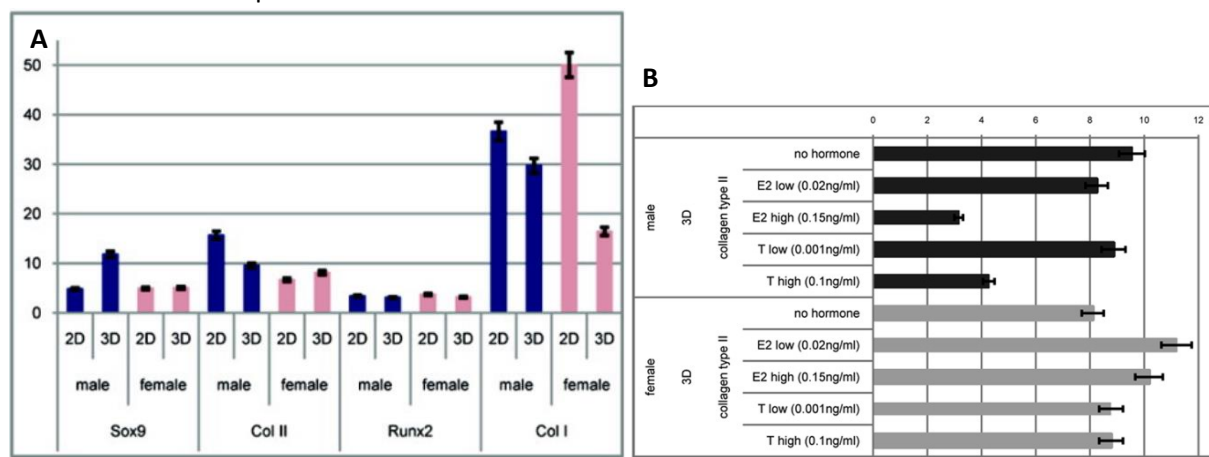


Figure 25. Sex differences of chondrogenic progenitor cells (CPCs) in late stage of OA. (A) Standardized level of expression for genes Sox9, COL2, Runx2, COL1 in monolayer and 3D culture in CPCs. (B) Standardized level of Col2 expression with treatment of two concentrations of 17 β -estradiol (E2) and testosterone (T). Expression differences were shown as binary logarithmic fold changes [14].

The same research investigated the involvement of sex hormones on gene expression in patients with late stage of knee OA. The hormones, testosterone and 17 β -estradiol (E2) were added in two concentrations. The influence of hormones on Col2 can be seen in Figure 25B. From this research can be concluded that E2 concentration influenced gene expressions of Col1, Col2, Runx2, Sox9, and ESR1 in CPC of females and males. For testosterone it has been observed that expression of Sox9, Runx2, Col1, Col2 was higher in CPCs of men. This suggests the challenge that hormones have a sex dependent effect on gene expression. Postmenopausal women have a decreased estrogen level resulting in higher risk of OA [14]. Therefore, as hormones influence gene expression, it is necessary to further elaborate on this aspect in future studies.

6.2.2. Future perspectives of the osteoarthritis-on-chip experiments

Currently, during cell extraction, the chondrocytes and osteoblasts were mixed. This hinders the investigation of individual gene expressions based on cell type. Increasing the size of the pillar that separates the cells is not a feasible option due to the important interaction of cells. An alternative solution is to consider a thin and sharp glass plate and place it exactly on the osteochondral barrier. This glass plate should penetrate the PDMS chip, and when collagenase is applied to the perfusion channels, the cells will remain on the corresponding side. However, finding a suitable glass piece that is both thin and sharp may be a challenge. Implementing this approach makes it more difficult to remove the cells from the chamber, which is already a challenging task. Therefore, careful consideration and investigation are required before proposing this idea.

The use of transcriptomics in research has increased in popularity over the last few years. With transcriptome data of human cells OA samples can be distinguished. Only one cell was necessary to create a single-cell transcriptome sequencing profile with over thousands of genes [44]. In research of OA and normal articular cartilage, 13,102 transcripts have been expressed in one sample. Different landscapes can be used for showing the results (Figure 26) [45]. If we can obtain these landscapes with differences between men and postmenopausal women in OA, a lot more genes can be investigated. Applying this tool in the future can expand the sex-specific profile. One of the limitations of this technique was that some silenced RNA or posttranscriptional gene silencing were measured, while they were not always translated into proteins [46].

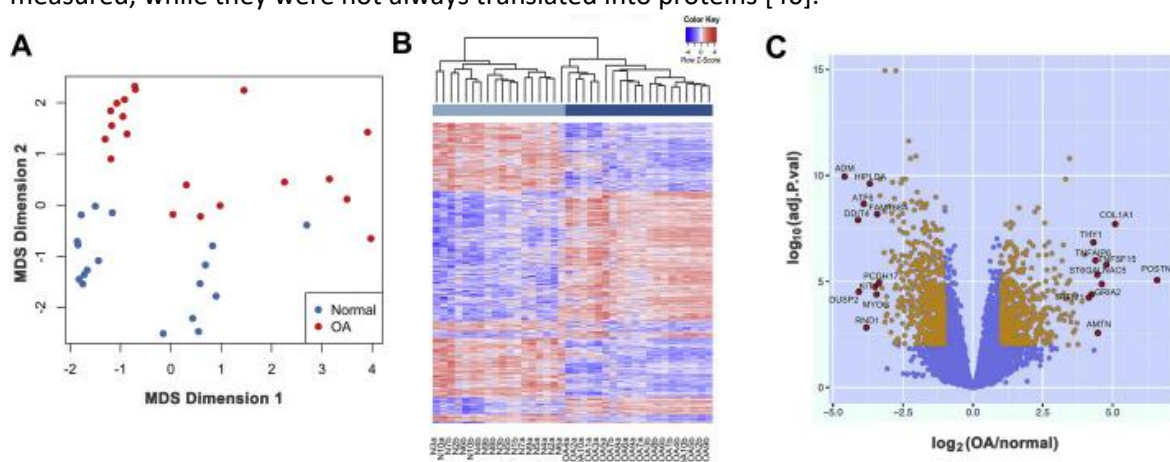


Figure 26. Transcriptomic landscape of normal and knee articular cartilage of OA. (A) Multidimensional scaling of gene expression. (B) Expression levels in heat map. (C) Volcano plate of gene expression [45].

This research focused on gene profiling of inflammatory cytokines in a three-day perfusion setup. By maintaining most parameters constant and varying only one variable, differences in gene expression parameters could be obtained. For example, future studies could extend the duration of the experiments to seven days and see if differences occur over a longer timeframe. Moreover, this experiment was part of a broader study, with the only variation being the inflammatory stimuli. Comparing the results of these studies can evaluate the influence of inflammatory cytokines on gene expression of the cells.

In a human joint, chondrocytes experience a combination of compression and shear strain. However, in the organ-on-a-chip device, the mechanical stimulation of a joint can only be implemented on uniaxial loading, either compression or stretching. To better mimic the physiological conditions inside the human body, a mechanical device can be integrated into the organ-on-a-chip system. Examples are the pushing air system (Figure 27A) [47] and the array of balloons (Figure 27B) [48]. This additional component would enable the application of multi-axial mechanical stimulation on cells [33, 47]. Implementing this system seems promising for the future.

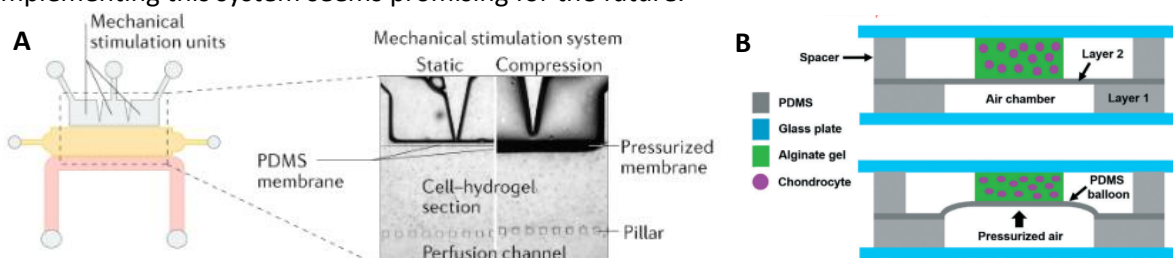


Figure 27. Tissue units for joint-on-tissue systems. Chondrocytes in hydrogel are exposed to pressure loading. (A) Mechanical unit generates multi-axial mechanical stimulation [47]. (B) Array of balloons with air pressure [48].

7. Conclusion

In this research we identified the genomic profile of sex-specific differences in an osteoarthritis-on-chip model. Specifically, we obtained a profile of 36 primers from one male and one postmenopausal female. The use of organ-on-a-chip technology allowed us to overcome limitations of existing models and advance our understanding of OA.

The holder designed in this research allows for simultaneous perfusion of multiple chips, enhancing research throughput, efficiency, and usability. In the design process of the holder, specific requirements and dimensions of all components are considered, resulting in a holder that proves to be useful in biological experiments. While the working of the holder operates properly, there are still opportunities for improvement and refinement.

The results obtained from analyzing RT-qPCR showed expressions of MMP1, MMP13, TGF β , VEGF, IL-6, CCL2, and RUNX2, which indicates the presence of OA. Moreover, a comparison between two donors indicated differences in gender expression. Certain genes, like ESR1, IL-1 β , MMP9, and RANKL, were expressed by the female donor but not the male donor. Conversely, SP7 and TLR4 were expressed by the male donor and not by the female donor (Figure 20). These findings suggest a potential gender-related difference in inflammation levels, supporting our initial hypothesis. However, other genes such as MMPs, TLRs, and IGFs were either not expressed or displayed minimal differences (Figure 18 and 19). To establish conclusive evidence regarding sex-related differences, future studies should aim to include a larger number of patients.

This study was part of a larger research project that investigated the influence of inflammatory stimuli on gene expression in an osteochondral-on-chip model. Moreover, the results imply that the gender differences observed in this model stimulated with pro-inflammatory cytokines, provide a starting point for understanding the mechanisms of gender specificity in OA. A complete understanding of gender differences in OA is crucial for the development of personalized and effective treatment strategies. Particularly because the global population ages and healthcare demands continue to rise.

8. References

- [1] Cieza A, Causey K, Kamenov K, Hanson SW, Chatterji S, Vos T. Global estimates of the need for rehabilitation based on the Global Burden of Disease study 2019: a systematic analysis for the Global Burden of Disease Study 2019. *Lancet*. 2021;396(10267):2006-17. doi: 10.1016/s0140-6736(20)32340-0.
- [2] Yao Q, Wu X, Tao C, Gong W, Chen M, Qu M, et al. Osteoarthritis: pathogenic signaling pathways and therapeutic targets. *Signal Transduct Target Ther*. 2023;8(1):56. doi: 10.1038/s41392-023-01330-w.
- [3] Evaluation IfHMa. Global Burden of Disease Collaborative Network. In: Washington Uo, editor. Global Burden of Disease Study 2019 (GBD 2019) results2020.
- [4] Hunter DJ, Bierma-Zeinstra S. Osteoarthritis. *The Lancet*. 2019;393(10182):1745-59. doi: 10.1016/S0140-6736(19)30417-9.
- [5] Tschon M, Contartese D, Pagani S, Borsari V, Fini M. Gender and Sex Are Key Determinants in Osteoarthritis Not Only Confounding Variables. A Systematic Review of Clinical Data. *J Clin Med*. 2021;10(14). doi: 10.3390/jcm10143178.
- [6] Contartese D, Tschon M, De Mattei M, Fini M. Sex Specific Determinants in Osteoarthritis: A Systematic Review of Preclinical Studies. *Int J Mol Sci*. 2020;21(10). doi: 10.3390/ijms21103696.
- [7] Sophia Fox AJ, Bedi A, Rodeo SA. The Basic Science of Articular Cartilage: Structure, Composition, and Function. *Sports Health*. 2009;1(6):461-8. doi: 10.1177/1941738109350438.
- [8] Nordin M, Victor FH. *Basic Biomechanics of the Musculoskeletal System*. 4th ed. Lippincott Williams & Wilkins; 2012.
- [9] Alford JW, Cole BJ. Cartilage restoration, part 1: basic science, historical perspective, patient evaluation, and treatment options. *Am J Sports Med*. 2005;33(2):295-306. doi: 10.1177/0363546504273510.
- [10] Goldring MB, Otero M. Inflammation in osteoarthritis. *Current Opinion in Rheumatology*. 2011;23(5):471-8. doi: 10.1097/BOR.0b013e328349c2b1.
- [11] Buckwalter JA, Mow VC, Ratcliffe A. Restoration of Injured or Degenerated Articular Cartilage. *JAAOS - Journal of the American Academy of Orthopaedic Surgeons*. 1994;2(4). doi: 10.5435/00124635-199407000-00002.
- [12] Glyn-Jones S, Palmer AJ, Agricola R, Price AJ, Vincent TL, Weinans H, et al. Osteoarthritis. *Lancet*. 2015;386(9991):376-87. doi: 10.1016/s0140-6736(14)60802-3.
- [13] Pan Q, O'Connor MI, Coutts RD, Hyzy SL, Olivares-Navarrete R, Schwartz Z, et al. Characterization of osteoarthritic human knees indicates potential sex differences. *Biology of Sex Differences*. 2016;7(1):27. doi: 10.1186/s13293-016-0080-z.
- [14] Koelling S, Miosge N. Sex differences of chondrogenic progenitor cells in late stages of osteoarthritis. *Arthritis & Rheumatism*. 2010;62(4):1077-87. doi: 10.1002/art.27311.
- [15] Hawker GA. Osteoarthritis is a serious disease. *Clin Exp Rheumatol*. 2019;37 Suppl 120(5):3-6.
- [16] Felson DT, Zhang Y, Hannan MT, Naimark A, Weissman BN, Aliabadi P, et al. The incidence and natural history of knee osteoarthritis in the elderly. The Framingham Osteoarthritis Study. *Arthritis Rheum*. 1995;38(10):1500-5. doi: 10.1002/art.1780381017.
- [17] Daniel P-A, Andrew J, Javaid MK, Cyrus C, Adolfo D-P, Nigel KA. Incidence and risk factors for clinically diagnosed knee, hip and hand osteoarthritis: influences of age, gender and

- osteoarthritis affecting other joints. *Annals of the Rheumatic Diseases*. 2014;73(9):1659. doi: 10.1136/annrheumdis-2013-203355.
- [18] Oliveria SA, Felson DT, Reed JI, Cirillo PA, Walker AM. Incidence of symptomatic hand, hip, and knee osteoarthritis among patients in a health maintenance organization. *Arthritis & Rheumatism*. 1995;38(8):1134-41. doi: 10.1002/art.1780380817.
- [19] Johnson VL, Hunter DJ. The epidemiology of osteoarthritis. *Best Practice & Research Clinical Rheumatology*. 2014;28(1):5-15. doi: 10.1016/j.berh.2014.01.004.
- [20] Peshkova M, Lychagin A, Lipina M, Di Matteo B, Anzillotti G, Ronzoni F, et al. Gender-Related Aspects in Osteoarthritis Development and Progression: A Review. *International Journal of Molecular Sciences*. 2022;23(5):2767. doi: 10.3390/ijms23052767.
- [21] Hanna FS, Teichtahl AJ, Wluka AE, Wang Y, Urquhart DM, English DR, et al. Women have increased rates of cartilage loss and progression of cartilage defects at the knee than men: a gender study of adults without clinical knee osteoarthritis. *Menopause*. 2009;16(4):666-70. doi: 10.1097/gme.0b013e318198e30e.
- [22] Boyan BD, Hart DA, Enoka RM, Nicoletta DP, Resnick E, Berkley KJ, et al. Hormonal modulation of connective tissue homeostasis and sex differences in risk for osteoarthritis of the knee. *Biol Sex Differ*. 2013;4(1):3. doi: 10.1186/2042-6410-4-3.
- [23] Key TJ, Allen NE, Verkasalo PK, Banks E. Energy balance and cancer: the role of sex hormones. *Proceedings of the Nutrition Society*. 2001;60(1):81-9. doi: 10.1079/PNS200068.
- [24] Klein SL, Flanagan KL. Sex differences in immune responses. *Nat Rev Immunol*. 2016;16(10):626-38. doi: 10.1038/nri.2016.90.
- [25] Srikanth VK, Fryer JL, Zhai G, Winzenberg TM, Hosmer D, Jones G. A meta-analysis of sex differences prevalence, incidence and severity of osteoarthritis. *Osteoarthritis Cartilage*. 2005;13(9):769-81. doi: 10.1016/j.joca.2005.04.014.
- [26] Deng ZH, Li YS, Gao X, Lei GH, Huard J. Bone morphogenetic proteins for articular cartilage regeneration. *Osteoarthritis and Cartilage*. 2018;26(9):1153-61. doi: 10.1016/j.joca.2018.03.007.
- [27] Xue X-T, Zhang T, Cui S-J, He D-Q, Wang X-D, Yang R-L, et al. Sexual dimorphism of estrogen-sensitized synoviocytes contributes to gender difference in temporomandibular joint osteoarthritis. *Oral Diseases*. 2018;24(8):1503-13. doi: 10.1111/odi.12905.
- [28] Nelson AE, Fang F, Shi XA, Kraus VB, Stabler T, Renner JB, et al. Failure of serum transforming growth factor-beta (TGF-beta1) as a biomarker of radiographic osteoarthritis at the knee and hip: a cross-sectional analysis in the Johnston County Osteoarthritis Project. *Osteoarthritis Cartilage*. 2009;17(6):772-6. doi: 10.1016/j.joca.2008.11.010.
- [29] Yu S, Sun L, Liu L, Jiao K, Wang M. Differential expression of IGF1, IGFR1 and IGFBP3 in mandibular condylar cartilage between male and female rats applied with malocclusion. *Journal of Oral Rehabilitation*. 2012;39(10):727-36. doi: 10.1111/j.1365-2842.2012.02332.x.
- [30] Pisitkun P, Deane JA, Difilippantonio MJ, Tarasenko T, Satterthwaite AB, Bolland S. Autoreactive B cell responses to RNA-related antigens due to TLR7 gene duplication. *Science*. 2006;312(5780):1669-72. doi: 10.1126/science.1124978.
- [31] Aomatsu M, Kato T, Kasahara E, Kitagawa S. Gender difference in tumor necrosis factor- α production in human neutrophils stimulated by lipopolysaccharide and interferon- γ . *Biochem Biophys Res Commun*. 2013;441(1):220-5. doi: 10.1016/j.bbrc.2013.10.042.

- [32] Torcia MG, Nencioni L, Clemente AM, Civitelli L, Celestino I, Limongi D, et al. Sex Differences in the Response to Viral Infections: TLR8 and TLR9 Ligand Stimulation Induce Higher IL10 Production in Males. *PLOS ONE*. 2012;7(6):e39853. doi: 10.1371/journal.pone.0039853.
- [33] Banh L, Cheung KK, Chan MWY, Young EWK, Viswanathan S. Advances in organ-on-a-chip systems for modelling joint tissue and osteoarthritic diseases. *Osteoarthritis and Cartilage*. 2022;30(8):1050-61. doi: 10.1016/j.joca.2022.03.012.
- [34] Samvelyan HJ, Hughes D, Stevens C, Staines KA. Models of Osteoarthritis: Relevance and New Insights. *Calcified Tissue International*. 2021;109(3):243-56. doi: 10.1007/s00223-020-00670-x.
- [35] Bhatia SN, Ingber DE. Microfluidic organs-on-chips. *Nature Biotechnology*. 2014;32(8):760-72. doi: 10.1038/nbt.2989.
- [36] Paggi CA, Teixeira LM, Le Gac S, Karperien M. Joint-on-chip platforms: entering a new era of in vitro models for arthritis. *Nature Reviews Rheumatology*. 2022;18(4):217-31. doi: 10.1038/s41584-021-00736-6.
- [37] Pocha C. Lean Six Sigma in Health Care and the Challenge of Implementation of Six Sigma Methodologies at a Veterans Affairs Medical Center. *Quality Management in Healthcare*. 2010;19(4). doi: 10.1097/QMH.0b013e3181fa0783.
- [38] Miranda E. MoSCoW Rules: A quantitative exposé (Accepted for presentation at XP2022). 2021.
- [39] Serdar CC, Cihan M, Yücel D, Serdar MA. Sample size, power and effect size revisited: simplified and practical approaches in pre-clinical, clinical and laboratory studies. *Biochem Med (Zagreb)*. 2021;31(1):010502. doi: 10.11613/bm.2021.010502.
- [40] Perruccio AV, Badley EM, Power JD, Canizares M, Kapoor M, Rockel J, et al. Sex differences in the relationship between individual systemic markers of inflammation and pain in knee osteoarthritis. *Osteoarthritis and Cartilage Open*. 2019;1(1):100004. doi: 10.1016/j.ocarto.2019.100004.
- [41] Galateanu B, Hudita A, Biru EI, Iovu H, Zaharia C, Simsensohn E, et al. Applications of Polymers for Organ-on-Chip Technology in Urology. *Polymers (Basel)*. 2022;14(9). doi: 10.3390/polym14091668.
- [42] Chao P, Maguire T, Novik E, Cheng KC, Yarmush ML. Evaluation of a microfluidic based cell culture platform with primary human hepatocytes for the prediction of hepatic clearance in human. *Biochem Pharmacol*. 2009;78(6):625-32. doi: 10.1016/j.bcp.2009.05.013.
- [43] Vollertsen AR, de Boer D, Dekker S, Wesselink BAM, Haverkate R, Rho HS, et al. Modular operation of microfluidic chips for highly parallelized cell culture and liquid dosing via a fluidic circuit board. *Microsystems & Nanoengineering*. 2020;6(1):107. doi: 10.1038/s41378-020-00216-z.
- [44] Li C, Zheng Z. Cartilage Targets of Knee Osteoarthritis Shared by Both Genders. *International Journal of Molecular Sciences*. 2021;22(2):569. doi: 10.3390/ijms22020569.
- [45] Fisch KM, Gamini R, Alvarez-Garcia O, Akagi R, Saito M, Muramatsu Y, et al. Identification of transcription factors responsible for dysregulated networks in human osteoarthritis cartilage by global gene expression analysis. *Osteoarthritis and Cartilage*. 2018;26(11):1531-8. doi: 10.1016/j.joca.2018.07.012.
- [46] Scanlan LD, Wu KL. Systems biology application in toxicology: Steps toward next generation risk assessment in regulatory toxicology. *Reference Module in Biomedical Sciences*. Elsevier; 2023.

- [47] Paggi CA, Venzac B, Karperien M, Leijten JCH, Le Gac S. Monolithic microfluidic platform for exerting gradients of compression on cell-laden hydrogels, and application to a model of the articular cartilage. *Sensors and Actuators B: Chemical*. 2020;315:127917. doi: 10.1016/j.snb.2020.127917.
- [48] Lee D, Erickson A, You T, Dudley AT, Ryu S. Pneumatic microfluidic cell compression device for high-throughput study of chondrocyte mechanobiology. *Lab on a Chip*. 2018;18(14):2077-86. doi: 10.1039/C8LC00320C.
- [49] Jung B, Seo KS, Kwon SJ, Lee K, Hong S, Seo H, et al. Efficacy evaluation of syringe pump developed for continuous drug infusion. *J Dent Anesth Pain Med*. 2016;16(4):303-7. doi: 10.17245/jdapm.2016.16.4.303.
- [50] Infusetek D. Syringe pumps DK Infusetek Catalog 2023. In: Drifton, editor. Qingpu District, Shanghai2023.
- [51] Leung CM, de Haan P, Ronaldson-Bouchard K, Kim G-A, Ko J, Rho HS, et al. A guide to the organ-on-a-chip. *Nature Reviews Methods Primers*. 2022;2(1):33. doi: 10.1038/s43586-022-00118-6.
- [52] Chandran Suja V, Frostad JM, Fuller GG. Impact of Compressibility on the Control of Bubble-Pressure Tensiometers. *Langmuir*. 2016;32(46):12031-8. doi: 10.1021/acs.langmuir.6b03258.
- [53] Ye R: CNC Machining Materials – How to Choose One for Your CNC Milling Applications? (2018). Accessed June 1 2023.
- [54] Zhang P, Liu Z. Plastic deformation and critical condition for orthogonal machining two-layered materials with laser cladded Cr-Ni-based stainless steel onto AISI 1045. *Journal of Cleaner Production*. 2017;149:1033-44. doi: 10.1016/j.jclepro.2017.02.167.

9. Appendix

9.1. The holder system

9.1.1. Specifications of pump

For this research, a SPLab10 syringe pump will be utilized (Figure 28B). The pump has compact dimensions and has previously been used in related research. The syringe pump offers precise control over pressure, making it suitable for handling liquids. It enables the user to define the total volume of fluid and deliver it at an accurate speed [49, 50].

The pump offers possible pumping systems: the withdrawal mode and the infusion mode, each suitable for different applications (Figure 28A) [50]. The infusion, also known as the pushing system, delivers the perfusion from the syringe pump through the chip into the waste tube. On the other hand, the withdrawal system works in reverse. It starts the perfusion within the tube, while the pump pulls the medium through the chip, with the waste being collected inside the syringe. This approach allows for the implementation of a larger starting volume as the syringe pump has a maximum capacity of 10 mL. Consequently, experiments can run for a longer period without the need for medium refreshment. However, this approach presents challenges in waste analyses because the waste needs to be transferred to an appropriate tube for storage and analysis. Additionally, storing and cleaning of syringes will be more complicated, and there is an increased risk of syringe leaking, which is undesirable.

During device operations, air bubbles may occur, especially when connecting a new syringe filled with medium. These bubbles can come into direct contact with cells or can block the perfusion flow, potentially causing damage to the cells [51]. Therefore, preventing this phenomenon is crucial. Although research suggests that air bubbles are more common in infusion systems [52], previous research with the infusion setup did not encounter any issues. Overall, the infusion system is considered more favorable due to its easier collection of conditioned media.

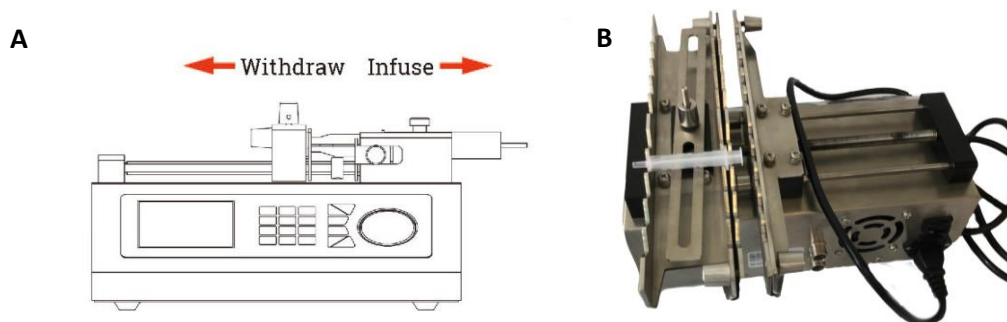


Figure 28. Laboratory syringe pump working principle of the SPLab10. (A) Schematic sketch with withdraw and infusion mode [50]. (B) Illustration of pump used in the experiments.

9.1.2. Specification of organ-on-chips direction

Another important specification is the direction of the organs-on-a-chip, which influences the design of the chip-holder. There are three different options for the flow direction based on the orientation of the chips and the microscope slide, as illustrated in Figure 29. Option A corresponds to the current orientation of the chips on the microscope slide, where the chips are placed horizontally and the slide vertically. In this configuration, there is no crosstalk between the tubing. However, for the other two options, the chips need to be rotated by 90 degrees. In these orientations there is a significant amount of crosstalk between the tubing. This crosstalk occurs when multiple tubing lines converge, resulting in interference between the flows. To address the crosstalk issue, one chip can be placed on each microscope slide. However, this solution is not ideal. Therefore, option A is the better choice as it eliminates crosstalk.

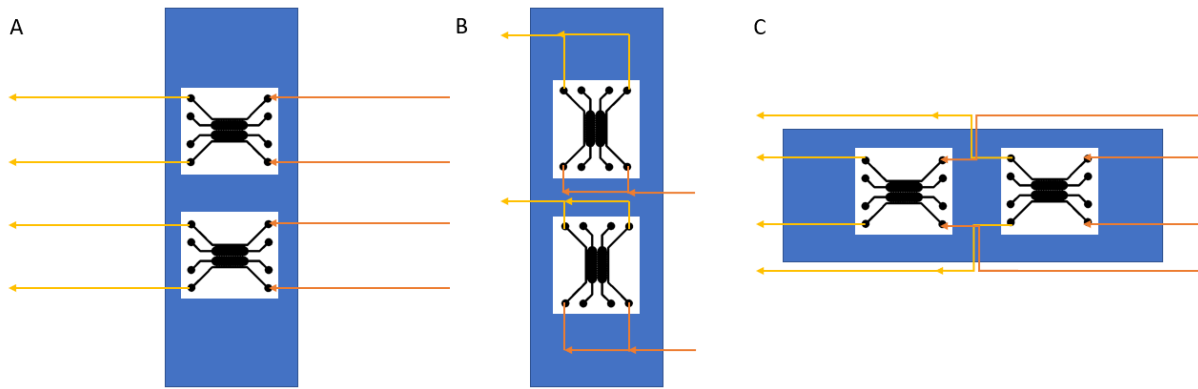


Figure 29. Three possible chips and microscope slide direction and their influence on the flow. The inlet tubing is shown in orange, and the outlet tubing in yellow. (A) The chips are placed horizontally and the slide vertically, ensuring no crosstalk between the tubing. (B) The chips and slides are placed vertically. In this orientation, there is significant crosstalk between the tubing lines. (C) The chips and slide are placed horizontally, resulting in high degree of crosstalk between the tubing lines.

9.1.3. Concept development

Three chip-holder concepts are developed using SolidWorks and presented in Table 4. Concepts 2 and 3 are smaller and both use the flow direction sketched in Figure 29C. However, a potential issue with these concepts is the occurrence of crosstalk among the tubing lines. To carefully support the perfusion of the chips, it is necessary to minimize the congestion of tubing. An alternative solution is presented in concept 1, which is slightly wider than the other two concepts. In this design, two chips can be placed in their original orientation, allowing for the maximum capacity without tubing crosstalk. Therefore, concept 1 appears to be the most suitable option.

In option 1, ten chips can be fully perfused when using a splitter positioned right after the syringes. The medium will be split into two inlets. However, for this research, the splitter will not be used, and only five chips will be studied from each donor.

Regarding the waste tube holder, two concepts are developed and presented in Table 5. Both concepts feature holes of varied sizes for 2 mL tubes and 15 mL tubes. The user can choose the preferred tube size based on the experiment's duration. It is not feasible to include more holes due to the width of the baseplate, which cannot exceed 450 mm because of the incubator dimensions.

The primary difference between the two concepts lies in their connection to the baseplate and chip-holder. Concept 1 provides a stable holder that can be placed on the surface after transportation. The production and fixation of concept 1 is more challenging compared to concept 2, which is connected to the support rib of the chip-holder via triangles. The only drawback of concept 2 is that it cannot stand on its own after being transported to another location. However, considering the high complexity of concept 1 and the research timeframe, concept 2 is more favorable.

Table 4. Three chip-holder concepts, presented in an isometric view and top view using SolidWorks. The flow direction, as explained in Figure 29, is also shown. The advantages and drawbacks are taken into consideration when selecting the appropriate chip-holder concept.

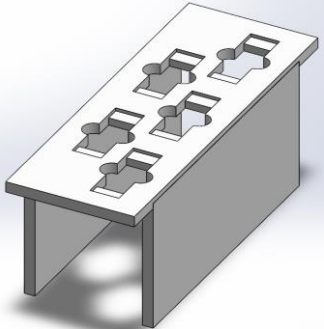
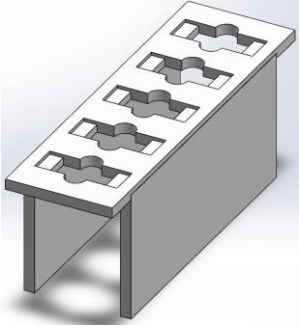
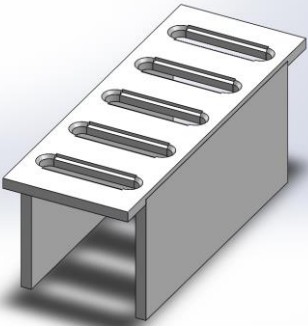
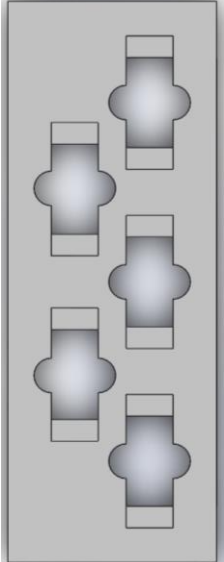
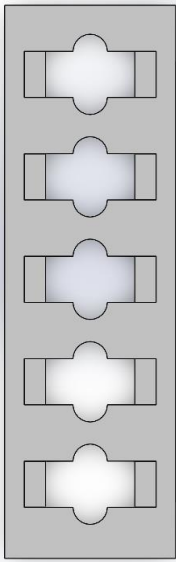
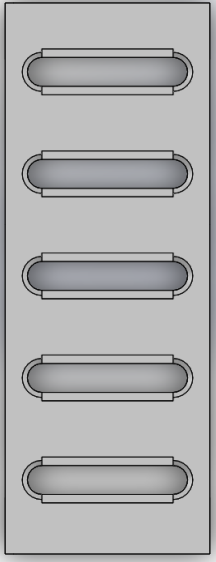
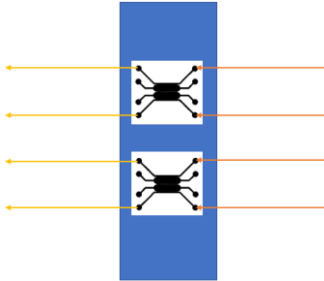
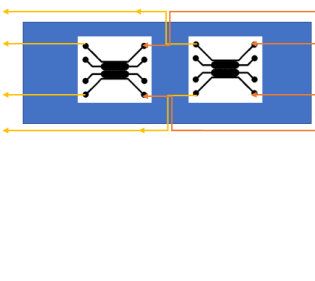
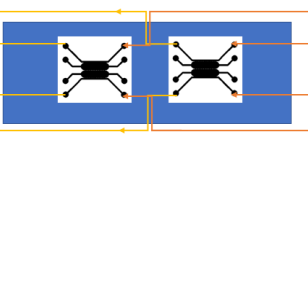
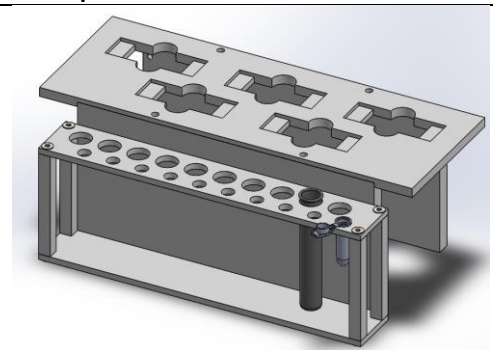
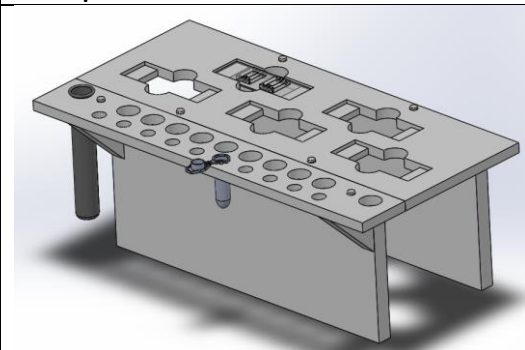
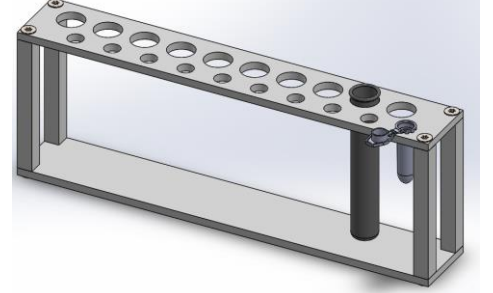
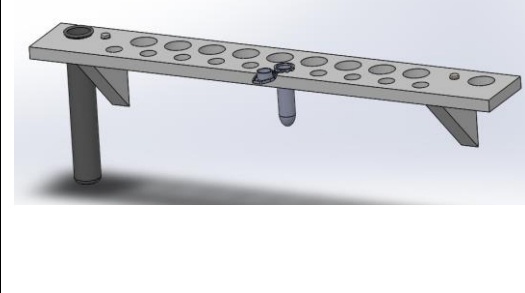
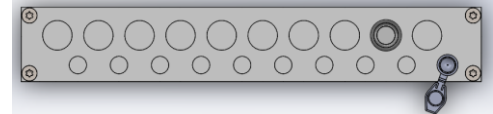
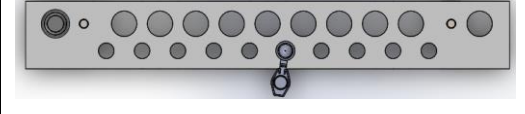
	Concept 1	Concept 2	Concept 3
Isometric view			
Top view			
Flow direction			
Advantages	<ul style="list-style-type: none"> • No need to adjust the current placement of chips • Low chance of tubing crosstalk 	<ul style="list-style-type: none"> • Smaller chip-plate, resulting in a compact baseplate that fits easily in the incubator 	<ul style="list-style-type: none"> • Easier production process
Drawbacks	<ul style="list-style-type: none"> • More complex in production compared to the other concepts 	<ul style="list-style-type: none"> • Increased risk of tube crosstalk when using two chips on each microslide 	<ul style="list-style-type: none"> • Increased risk of tube crosstalk when using two chips on each microslide • Complex fixation of chips in the horizontal direction

Table 5. Two concepts are presented for the waste tube holder, both created in SolidWorks. The table includes isometric views of each concept with and without the chip-holder, as well as the top view. The advantages and drawbacks of each concept are provided.

	Concept 1	Concept 2
Isometric view with chip-holder		
Isometric view of waste tube holder		
Top view of waste tube holder		
Advantages	<ul style="list-style-type: none"> • Tube holder can be removed as a whole and placed in a stable location 	<ul style="list-style-type: none"> • Relatively easier production process • Triangle blocks are fixed to the support plate, and the top plate can be easily taken out.
Withdraws	<ul style="list-style-type: none"> • Fixation of the holder is more challenging • Complex production process 	<ul style="list-style-type: none"> • When the tube holder is removed, it cannot stand on its own

9.1.4. Material choices

Various materials are considered for the design. A CNC machine allows the use of metals, plastics, woods, foams, ceramics, and composites. The focus is on metals and plastics due to environmental, availability, and cost factors. Metals provide excellent precision and ruggedness, but they can be costly and vulnerable to corrosion. Among the metals, aluminum (V-ID: 5561) is chosen for the baseplate due to its exceptional strength-to-weight ratio, excellent machinability, and lower cost compared to other materials. The baseplate requires greater strength to support the weight of the other components. Therefore, the other parts are produced using plastic, which is cost-effective and still offers sufficient strength [53], as these components do not need to be strong.

When it comes to CNC milling, one potential issue is the deformation of plastic at high temperatures, but the CNC machine does not reach high temperature [54]. Commonly used plastics include Polymethyl Methacrylate (PMMA) and Thermoplastic Polyvinyl Chloride (PVC). PMMA is transparent and has flexural and high tensile strength. It can resist organic solvents but is more expensive compared to PVC. On the other hand, PVC offers sturdiness, corrosion resistance, and fire resistance [53]. PVC was chosen since it is cheap and available in large quantities at the workshop. For the plates, we used V-ID number 5662 and V-ID number 5660. The color grey is chosen for these components, as no specific color criteria are set.

9.1.5. Production drawing of each compartment

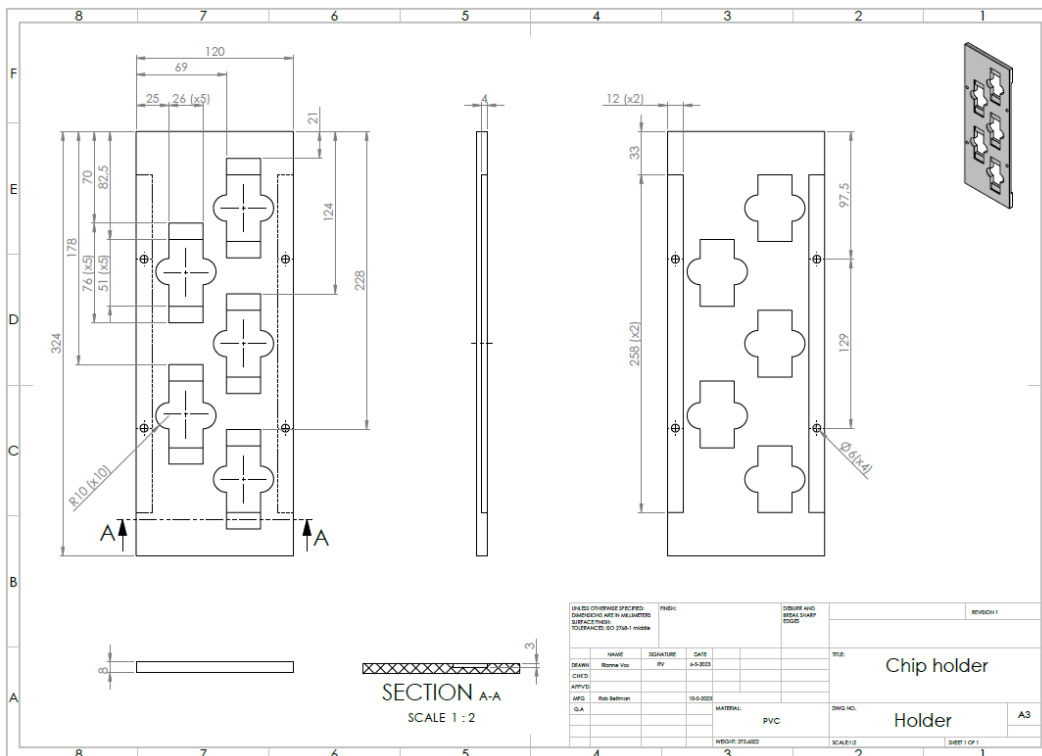


Figure 30. Drawing of chip-holder created in SolidWorks with dimensions in millimeters (mm). The drawing serves as reference for the sawing and milling production.

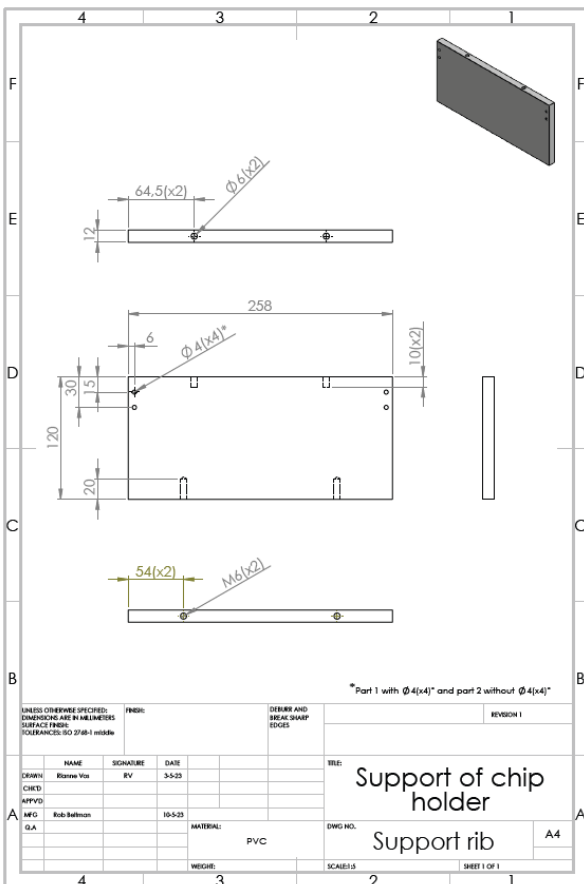


Figure 31. Drawing of the support ribs of the chip-holder created in SolidWorks with dimensions in millimeters (mm). The drawing serves as reference for the sawing, milling, and drilling production process.

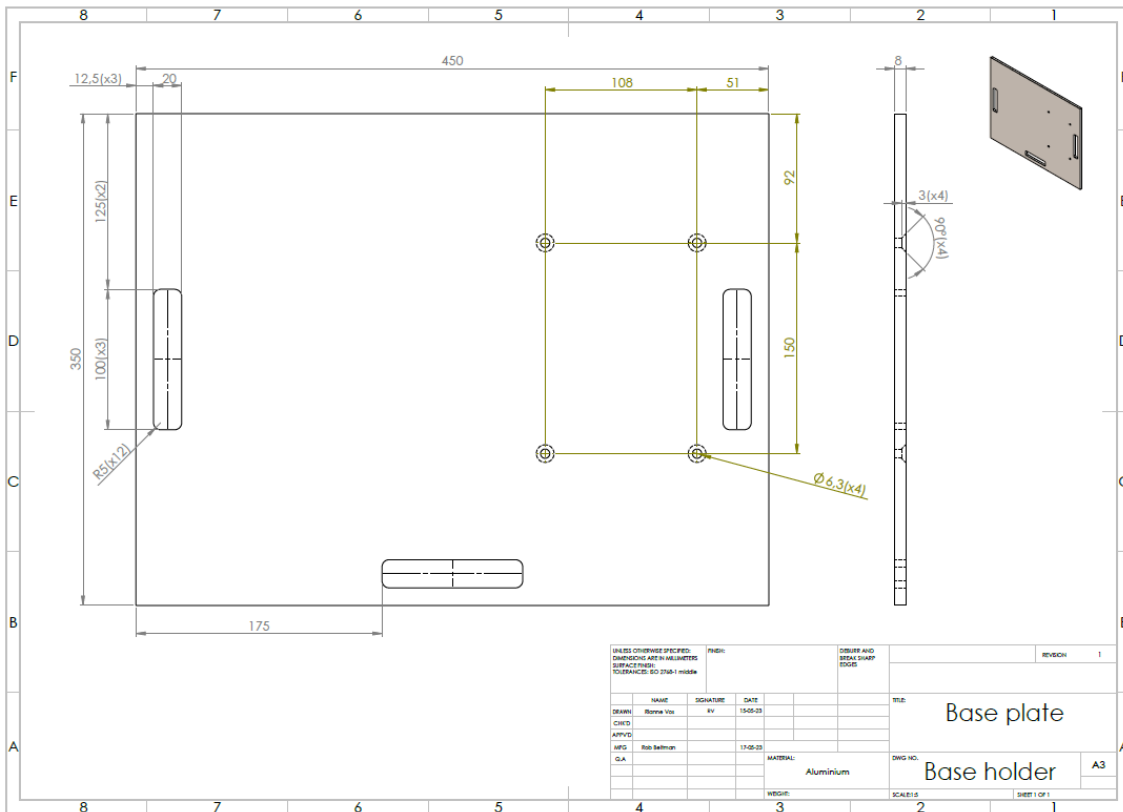


Figure 32. Drawing of baseplate created in SolidWorks with dimensions in millimeters (mm). The drawing serves as reference for the sawing and milling production process.

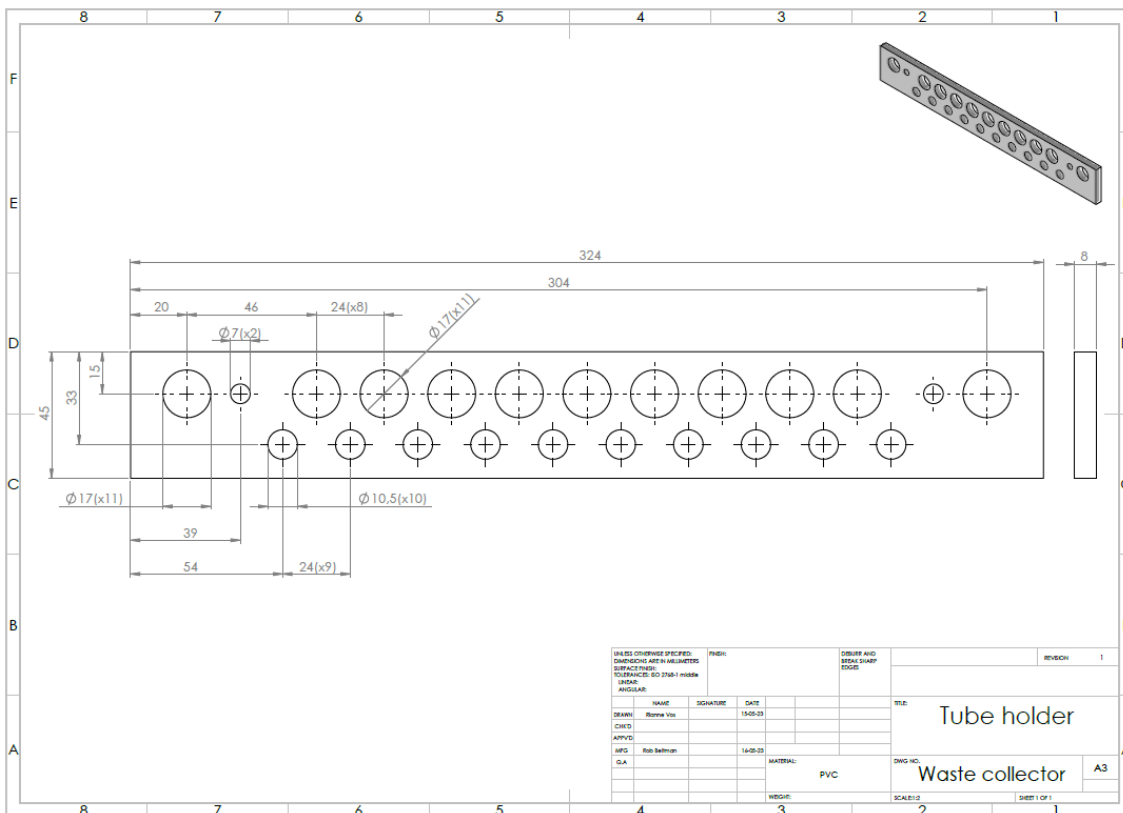


Figure 33. Drawing of waste tube plate created in SolidWorks with dimensions in millimeters (mm). The drawing serves as reference for the sawing, milling, and drilling production process.

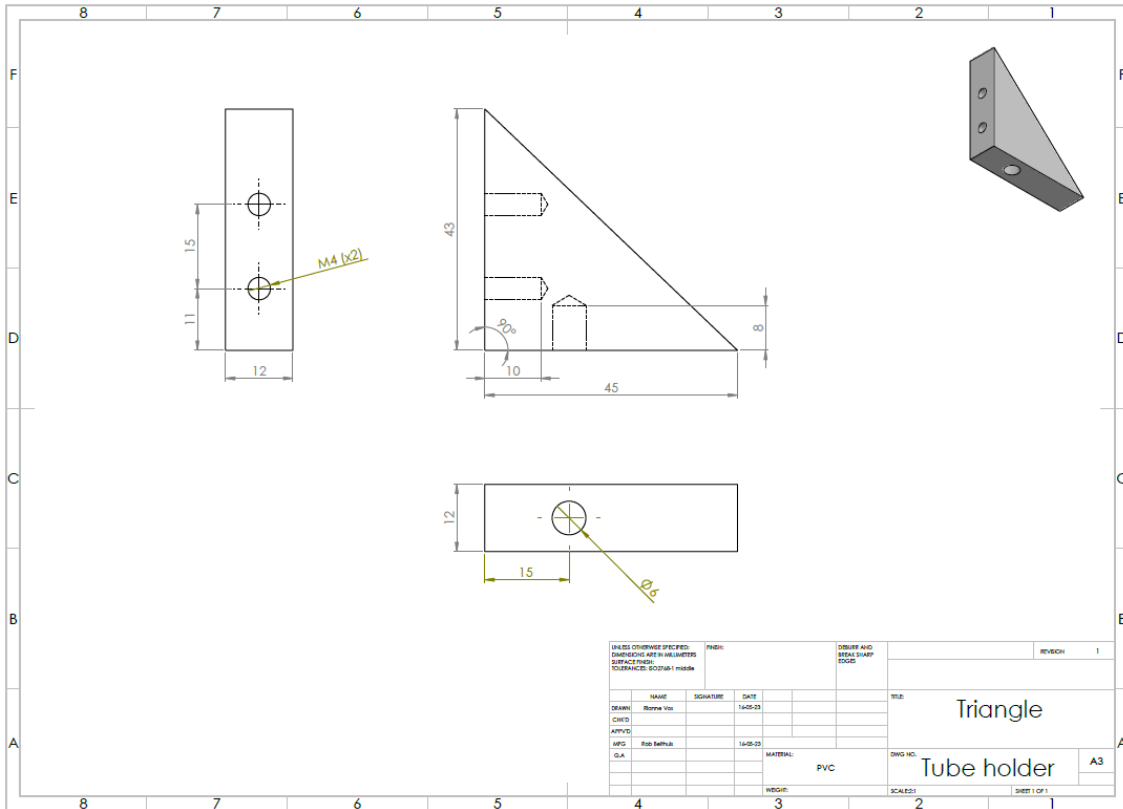


Figure 34. Drawing of triangles created in SolidWorks with dimensions in millimeters (mm). The drawing serves as reference for the sawing, milling, and drilling production process.

9.1.6. Final product

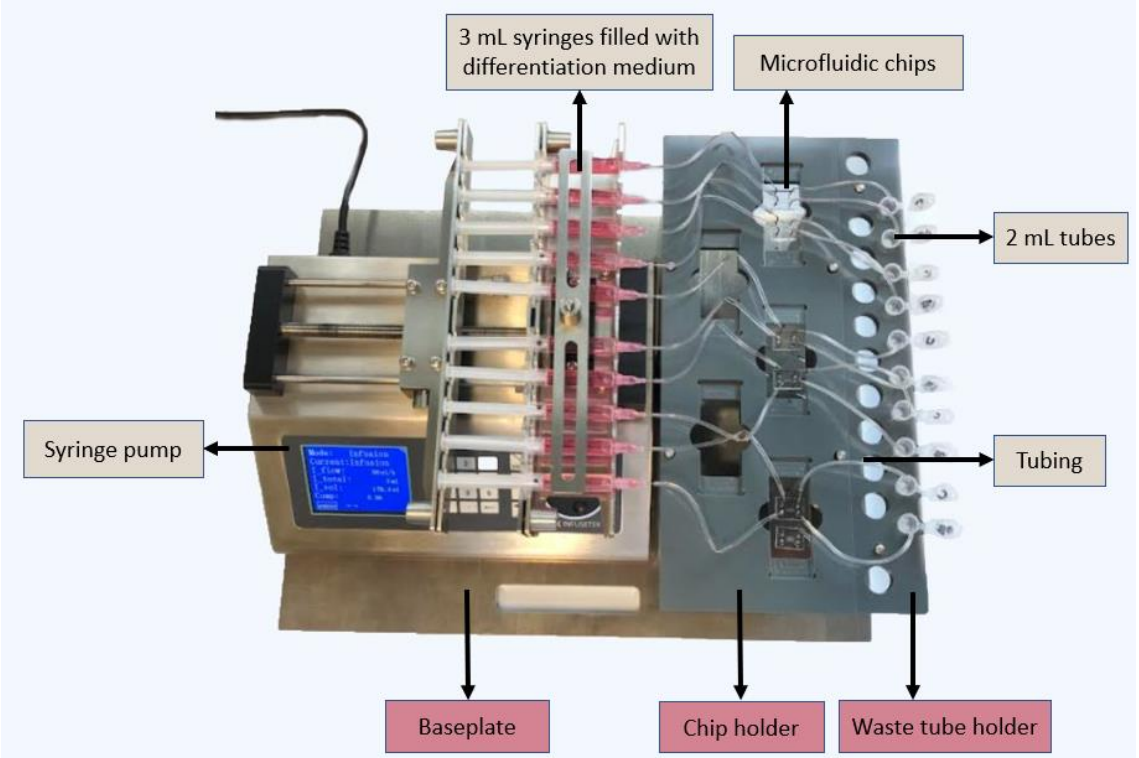


Figure 35. Design of final product with all components. This setup was obtained during the experiments. The deep pink components in the figure represent the parts designed, while the other components were already in the laboratory.

9.1.7. Revision on list-of-requirements

The final holder can be evaluated based on the aims and requirements set for its design. The color-coded system indicates the degree to which each aim or requirement has been achieved. The green color met the goal/requirements, while the orange color indicates partial fulfilment. A detailed explanation for each aim is provided below, along with the reasoning behind the color classification for the requirements (Table 6).

The holder aims was to;

- Increase the throughput of organs-on-chips.
The maximum of perfusion ten chips has been reached.
- Facilitate easier transport of microfluidics.
The design of the baseplate has made the transport of the system with the microfluidics easier.
- Maintain the syringe pump, tubing and microfluidic chips leveled to avoid high pressure differences during perfusion.
No instances of leaking or pressure issues were observed during the experiments, indicating successful maintenance of level.
- Minimize dead volume in the tubing by placing the chips and syringes close together.
The tubing was kept relatively short to minimize dead volume, reducing the chances of bubble formation during perfusion and minimizing the required volume of medium. The waste volume was also minimized to prevent significant dilution of secreted proteins.
- Collect conditioned media from each individual perfusion channel.
The waste tube holder was able to collect media from each perfusion channel individually.
- Provide independent accessibility of components.
The chip-holder and waste tube holder were designed for individual transportation. However, the waste tube holder cannot stand on its own as it lacks support. Additionally, the distances between the tubes were too large to fit inside a regular tube rack.
- Ensure long-term utilization of the holder.
The holder has been used in this research for three times of three days each. While it has the potential for longer-term utilization, its exact lifespan cannot be guaranteed with 100% certainty. The materials were expected to last for a considerable period. The primary limiting factor is the humidity of the pump, which should be kept below 80%.

Table 6. Revision of the list of requirements. All requirements were revised based on full (green) or partial (orange) fulfilment.

	Requirements	Reasoning of color	MoSC oW
Chip-holder			
1.1	The chip-holder shall provide five microscope slide places.	The holder consists of five microscope slide locations.	M
1.2	The chip-holder shall stabilize the microscope slides.	The slides were fixed inside the holes without tubing.	M
1.3	The microscope slides shall be pulled out from the chip-holder.	Finger holes were provided to facilitate the removal of slides from the chip-holder.	M
1.4	The chip-holder shall fit under the microscope.	It was possible to observe the chips inside the holder under a microscope, although focusing on the cells can be challenging due to the relatively thick plate.	S
1.5	The chip-holder shall contain openings to see the chips under the microscope.	The holes within the chip-holder were adequately sized for viewing the chips.	M

1.6	The chip-holder shall easily be disconnected from the baseplate.	The top-plate of the chip-holder can easily be detached from the baseplate with use of the pin connection.	M
1.7	The height of the chip-holder shall be lower than the height of syringe pump.	There was a small height difference in the preferred direction.	S
Waste tube holder			
2.1	The waste tube holder shall easily be disconnected from the baseplate.	The top-plate of the waste tube holder can easily be detached from the baseplate with use of the pin connection.	S
2.2	The waste tube holder shall be separate portable from the chip-holder.	The top-plate can be carried separately. Only, it cannot stand on its own or fit into a tube rack.	S
2.3	The waste tube holder shall fixate the tubes.	The holes were appropriately sized for 2 mL tubes, fitting them precisely.	S
2.4	The waste tube holder shall consist of a minimum of two different hole sizes.	The tube holder consists of two types of holes, 2 mL and 15 mL.	C
2.5	The reservoirs shall easily be removed from the waste tube holder.	Some reservoirs may be slightly tight within the holes due to material deformation.	M
Baseplate			
3.1	The baseplate shall fit inside the incubator.	The baseplate conveniently fits inside the incubator.	M
3.2	The height of the total holder, including the baseplate, shall be lower than 185 mm.	The height was lower than 185 mm.	M
3.3	The chip-holder and waste tube holder shall be detachable from the baseplate.	The top plates can be removed from the baseplate, while the support ribs with triangles remain attached.	S
3.4	The baseplate shall be able to carry the weight of the different parts.	The aluminum plate was strong enough to support the weight of the components.	M
3.5	The strength of the baseplate shall be able to carry the weight of the different parts.	The aluminum plate was strong enough to support the weight of the components.	M
3.6	The baseplate shall be transportable.	Handgrips were incorporated to facilitate transport, although the overall weight increased a lot by choosing aluminum as material.	S
3.7	The baseplate shall contain a minimum of three handgrips for transportation.	There were three handgrips located on the baseplate.	C
3.8	Everything shall be connected outside the incubator, except for the electrical pluck from the pump.	The entire holder fits inside the incubator, and the electrical pluck can be connected from outside.	M
Chips			
4.1	The chips shall only be placed on top of the microscope slides (76 x 26 mm).	In microscope slides fit into all holes without significant tolerances.	M
4.2	A maximum of two chips shall be placed on one microscope slide.	Two chips can be placed on a single slide and connected to the tubing.	C
4.3	The chips shall be placed above the holes from the chip-holder.	The location was not narrowed because the holes were appropriately sized.	M
4.4	The chips shall be connected to the syringes with tubing.	The connection between the chips and tubing was secure. To minimize dead volume, two tubing length options have been created.	M
4.5	The chips shall be connected to the waste tube holder with tubing.	When collecting conditioned media, we noticed that the stiffness of the tubing can lift the slides.	M
4.6	The tubing should be less crowded.	The tubing was well-organized, although it can be challenging to identify which tubing corresponds to each reservoir when placing the waste tube holder inside the incubator again.	S

9.1.8. Translation to industrial design

The translation of the holder into industrial design involved considering factors such as production scalability, automation, smart features, and material optimization. There will be big differences between the current holder design and the industrial design.

Table 7. Differences of holder in academic context and industrial design settings.

	Academic context	Industrial settings
Automated production	Produced by hand.	An automated production process would be preferred.
Consumed by	2 people	Multiple people
Live expansion	Will be used around 50 times and each time a couple of days (relative short).	Design needs to be robust because it will probably be used 24/7.
Material optimization	Basic research about material design is provided.	Material plays a crucial role in production. Extending the research might influence material choice.
Modular design	Only a newly designed top-plate can easily be changed. Otherwise, the total design needs to be reproduced.	Allows for customization and flexibility.
Smart features and connectivity	No features added to the design.	May include sensors for monitoring parameters such as temperature, pressure, or fluid level.
Upscaling of syringes	The maximum capacity of the pump is ten.	Upscaling above ten syringes is preferred to increase efficiency.

9.2. The osteoarthritis-on-chip model

9.2.1. Medium composition

Table 8. Components of chondrocyte proliferation medium and osteoblast proliferation medium.

	Reagent	Supplier	Reference	Stock	Final Concentration
Chondrocyte proliferation medium	DMEM High Glucose	Gibco	41965062	-	-
	Fetal Bovine Serum	Sigma	F7524-500ML	100%	10%
	Sodium Pyruvate	Gibco	11360070	100mM	1mM
	Penicillin/ Streptomycin	Gibco	15140130	1000U/mg/ mL	100U/mg/mL
	HEPES buffer	Gibco	15630049	1M	10mM
	Non-essential amino acids	Gibco	11140050	100x	1x
	Ascorbic Acid	Sigma	A8960-5G	200mM	0.2mM
	Proline	Sigma	P5607-25G	40mM	0.4mM
Osteoblast proliferation medium	MEM α , nucleosides	Gibco	22571020	-	-
	Fetal Bovine Serum	Sigma	F7524-500ML	100%	10%
	Penicillin/ Streptomycin	Gibco	15140130	1000U/mg/ mL	100U/mg/mL

Table 9. Components of chondrocyte differentiation medium and osteoblast differentiation medium.

	Reagent	Supplier	Reference	Stock	Final concentration
Chondrocyte differentiation medium	DMEM High Glucose	Gibco	41965062	-	-
	Penicillin/ Streptomycin	Gibco	15140130	10000 U/mL	100 U/mL
	Sodium Pyruvate	Gibco	11360070	100 mM	1 mM
	ITS Mixture	Gibco	41400045	100 X	1 X
	Ascorbic Acid	Sigma	A8960-5G	200 mM	0.2 mM
	Dexamethasone	Sigma	D4902-25MG	10^{-5} M	10^{-7} M
	TGFB3	Preprotech	100-36E	10 ng/mL	10 ug/mL
Osteoblast differentiation medium	MEM α , nucleosides	Gibco	22571020	-	-
	Penicillin/ Streptomycin	Gibco	15140130	10000 U/mL	100 U/mL
	Ascorbic Acid	Sigma	A8960-5G	200 mM	0.2 mM
	Dexamethasone	Sigma	D4902-25MG	10^{-5} M	10^{-7} M
	Beta-Glycerophosphate	Sigma	G9422-10G	1 M	10 mM

9.2.2. qPCR primers and plate layout

Table 10. Primer sequences used for qPCR.

	Gene Symbol	Accession number	Forward sequence	Reverse sequence
Matrix Remodeling	MMP1	NM_001145938.2	AAAGGGAATAAGTACTGGGC	CAGTGTTCCTCAGAAAGAG
	MMP9	NM_004994.3	AAGGATGGGAAGTACTGG	GCCAGAGAAGAAGAAAAG
	MMP13	NM_002427.4	AGGCTACAACCTGTTTCTTG	AGGTGTAGATAGGAAACATGAG
	COL1 α 1	NM_000088.4	GCTATGATGAGAAATCAACCG	TCATCTCCATTCTTCCAGG
	COL2 α 1	NM_033150.3	GAAGAGTGGAGACTACTGG	CAGATGTGTTTCTTCTCCTTG
Receptor	TGFBR1	NM_001130916.3	AGACAATGGTACTTGGACTC	GTACCAACAATCTCCATGTG
	BMPR1A	NM_004329.3	CATACTGGTTTCATAGCGG	ATAAGCCAATTTAAGCAGGG
	VDR	NM_000376.3	ATCTGGATCTGAGTGAAGAAG	TCTCTGAATCCTGGTATCATC
	ESR1	NM_000125.4	GGAGTGTACACATTTCTGTC	CAAAGTGTCTGTGATCTTGTC
Wnt Pathway	WNT3A	NM_033131	GCATCAAGATTGGCATCC	CTCCCTGGTAGCTTTGTC
	WNT5A	NM_001256105	ATTAATTCTGGCTCCACTTG	GGTTATTCATACCTAGCGAC
	CTNNB1	NM_001904.4	CAACTAAACAGGAAGGGATG	CACAGGTGACCACATTTATATC
	DKK1	NM_012242.4	GAATAAGTACCAGACCATTGAC	CCATTTTTGCAGTAATTCCC
	DKK2	NM_014421.3	AGAATCTAGGAAGACCACAC	CGTGTGGTGGTACAGACTTC
Growth Factors	TGFB1	NM_000660.7	AACCACAACGAAATCTATG	CTTTAACTTGAGCCTCAGC
	IGF1	NM_000618.5	CCCAGAAGGAAGTACATTTG	GTTTAACAGGTAACCTGTGC
	IGFR1	NM_000875.5	AAAGACAAAATCCCATCAG	TGCAGGAAATCTCAAAGAC
	VEGFA	NM_001204384.2	AATGTGAATGCAGACCAAAG	GACTTATACGGGATTTCTTG
Inflammatory Cytokines	TNF	NM_000594.4	AGGCAGTCAGATCATCTTC	TTATCTCTCAGCTCCACG
	IL1B	NM_000576.3	CTAACAGATGAAGTGCTCC	GGTCATTCTCCTGGAAGG
	IL6	NM_000600.5	GCAGAAAAGGCAAAGAATC	CTACATTTGACCGAAGAGC
	CXCL8 (IL8)	NM_000584.4	GTTTTGAAGAGGGCTGAG	TTTGCTTGAAGTTTCACTGG
	IL11	NM_000641.4	ACAGGGAAGGGTTAAAGG	CAAACACAGTTTATGTCCC
	IL18	NM_001243211.2	CCTTTAAGGAAATGAATCCTCC	CATCTTATTATCATGTCTGGG
Osteoclast	CCL2	NM_002982.4	AGACTAACCCAGAAACATCC	ATTGATTGCATCTGGCTG
	CSF1	NM_000757.6	TTAAGAAGGCATTTCTCCTG	CCTTGTATGCTTTCATAATC
Osteoblast/Chondrocytes	TNFSF11A/RANKL	NM_003701.4	TGCATCTGGAAATGTGAC	ACGATGATGTCGCC
	SOX9	NM_000346.4	CTCTGGAGACTTCTGAACG	AGATGTGCGTCTGCTC
	RUNX2	NM_001015051.4	AAGCTTGATGACTCTAAACC	TCTGTAATCTGACTCTGTCC
	SP7 (Osterix)	NM_001173467.3	TGAGGAGGAAGTTCACTATG	CATTAGTGCTTGTAAAGGGG
	ALPL	NM_000478.6	TCTTCACATTTGGTGGATAC	ATGGAGACATTCTCTCGTTC
TLRs	ACAN	NM_001135.4	CACCCATGCAATTTGAG	AGATCATCACCACACAGTC
	TLR4	NM_003266.4	GATTTATCCAGGTGTGAAATCC	TATTAAGGTAGAGAGGTGGC
	TLR7	NM_016562.4	AGATATAGGATCACTCCATGC	CTTCCAAAATGGAATGTAGAGG
	TLR9	NM_017442.4	AAATCCCTCATATCCTGTC	TTGTAATAACAGTTGCCGTC

Table 11. qPCR plate layout.

	1	2	3	4	5	6	7	8	9	10	11	12	13	14	15	16	17	18	19	20	
	Negative Control		Tube 1		Tube 2			Negative Control		Tube 1		Tube 2			Negative Control		Tube 1		Tube 2		
18S							18S							TNF							
ACAN							IL1B							VDR							
ALP							IL6							VEGFA							
BMPR							IL8							WNT3A							
CCL2							MMP 13							WNT5A							
COL1							MMP 1														
COL2							MMP 9														
CSF1							RUNX 2														
CTNB1							SOX9														
DKK1							SP7														
DKK2							TGFB1														
ESR1							TGFBR 1														
IGFR1							TLR4														
IGF1							TLR7														
IL11							TLR9														
IL18							RANK L														